Inorganic Chemistry

Article

pubs.acs.org/IC

Experimental and Theoretical Investigation for the Level of Conjugation in Carbazole-Based Precursors and Their Mono-, Di-, and Polynuclear Pt(II) Complexes

Rayya A. Al-Balushi,[†] Ashanul Haque,[†] Maharaja Jayapal,[†] Mohammed K. Al-Suti,[†] John Husband,[†] Muhammad S. Khan,*[,†] Olivia F. Koentjoro,[§] Kieran C. Molloy,[§] Jonathan M. Skelton,*[,§] and Paul R. Raithby*[,§]

[†]Department of Chemistry, Sultan Qaboos University, P.O. Box 36, Al Khod 123, Muscat, Sultanate of Oman

[§]Department of Chemistry, University of Bath, Claverton Down, Bath, Avon BA2 7AY, United Kingdom

Supporting Information

ABSTRACT: A series of trimethylsilyl-protected monoalkynes ($Me_3SiC{\equiv}C{-}R$) and bis-alkynes ($Me_3SiC{\equiv}C{-}R{-}C{\equiv}CSiMe_3$) incorporating carbazole spacer groups (R = carbazole-2-yl, carbazole-3-yl, carbazole-2,7-diyl, *N*-(2-ethylhexyl)carbazole-2,7-diyl, carbazole-3,6-diyl, *N*-(2-ethylhexyl)carbazole-3,6-diyl), together with the corresponding terminal monoalkynes ($H{-}C{\equiv}C{-}R$) and bis-alkynes ($H{-}C{\equiv}C{-}R{-}C{\equiv}C{-}H$), have been synthesized and characterized. The CuI-catalyzed dehydrohalogenation reaction between *trans*-$[(Ph)(Et_3P)_2PtCl]$, *trans*-$[(Et_3P)_2PtCl_2]$, and *trans*-$[(P^nBu_3)_2PtCl_2]$ and the terminal alkynes in $^iPr_2NH/CH_2Cl_2$ affords a series of Pt(II) mono- and diynes, while the dehydrohalogenation polycondensation reactions with *trans*-$[(P^nBu_3)_2PtCl_2]$ under similar reaction conditions yields four Pt(II) poly-ynes of the form *trans*-$[(P^nBu_3)_2Pt{-}C{\equiv}C{-}R{-}C{\equiv}C{-}]_n$. The acetylide-functionalized carbazole ligands and the mono-, di-, and polynuclear Pt(II) σ-acetylide complexes have been characterized spectroscopically, with a subset analyzed using single-crystal X-ray diffraction. The Pt(II) mono-, di-, and poly-ynes incorporating the carbazole spacers are soluble in common organic solvents, and solution absorption spectra show a consistent red-shift between the 2- and 2,7- as well as 3- and 3,6-carbazole complexes. Computational modeling is used to explain the observed spectral shifts, which are related to the enhanced electronic delocalization in the latter systems. These results also indicate that the inclusion of carbazole-2,7-diyl units into rigid-rod organometallic polymers should enhance electronic transport along the chains.

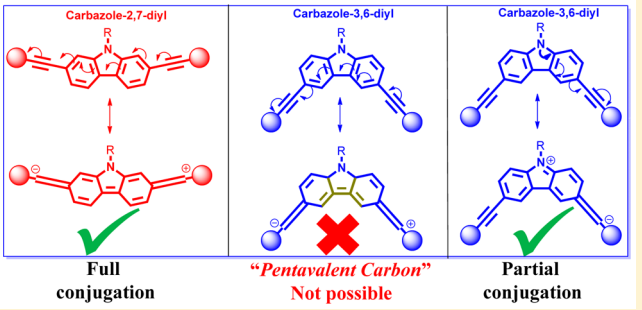

INTRODUCTION

The last few decades have seen a huge research effort in the pursuit of developing novel materials with enhanced optoelectronic properties.[1] Metal−organic frameworks (MOFs), especially conjugated organometallic compounds, have attracted considerable attention due to their potential applications in the modern materials industry (e.g., photovoltaic cells, field-effect transistors, light-emitting diodes, and nonlinear optics).[1c,d,2] One of the most promising systems is the *rigid-rod* type Pt(II) poly-ynes, *trans*-$[{-}Pt(P^nBu_3)_2{-}C{\equiv}C{-}R{-}C{\equiv}C{-}]_n$, where R is one of a number of aromatic, heteroaromatic, or mixed-heterocycle spacer groups.[3] A particularly attractive feature of the Pt(II) poly-ynes is the ability to fine-tune their optoelectronic properties by variation of the spacer groups.[4] Whereas the spacer plays an important role in determining the physicochemical properties of the materials, the Pt(II) ion plays a crucial role in controlling the photophysical properties.[5] It is well-known that triplet (T_x) states play an important role in the optoelectronic processes of conjugated polymers,[6] and the incorporation of Pt(II) into the polymer backbone populates the T_1 excited states by intersystem crossing, allowing for light emission from the decay of these states. Synthetic flexibility and compatibility with different conjugated spacers thus together allow fine control over the photophysical properties.[4b−e,7]

Among the more electron-rich of the reported spacers used in Pt(II) poly-ynes is the carbazole unit (Chart 1). This moiety provides a rigid planar biphenyl unit within the polymer backbone and facile functionalization via the N atom, offering

Chart 1. Carbazole Spacer Unit, with the Numbering Scheme Adopted in This Work Indicated

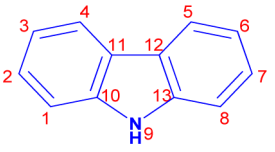

Received: March 1, 2016

DOI: 10.1021/acs.inorgchem.6b00523
Inorg. Chem. XXXX, XXX, XXX−XXX

Scheme 1. Comparison of Synthetic Routes to Alkylated Carbazoles Using NaH and KO^{t}Bu

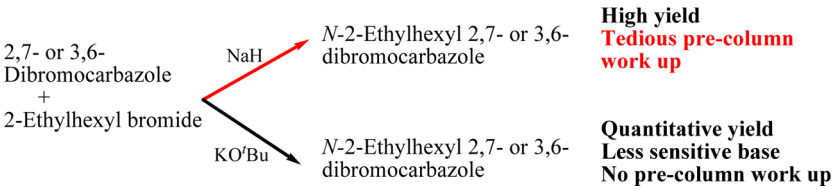

Scheme 2. Syntheses of Mono- and Bis-Acetylide-Functionalized Carbazole Ligands

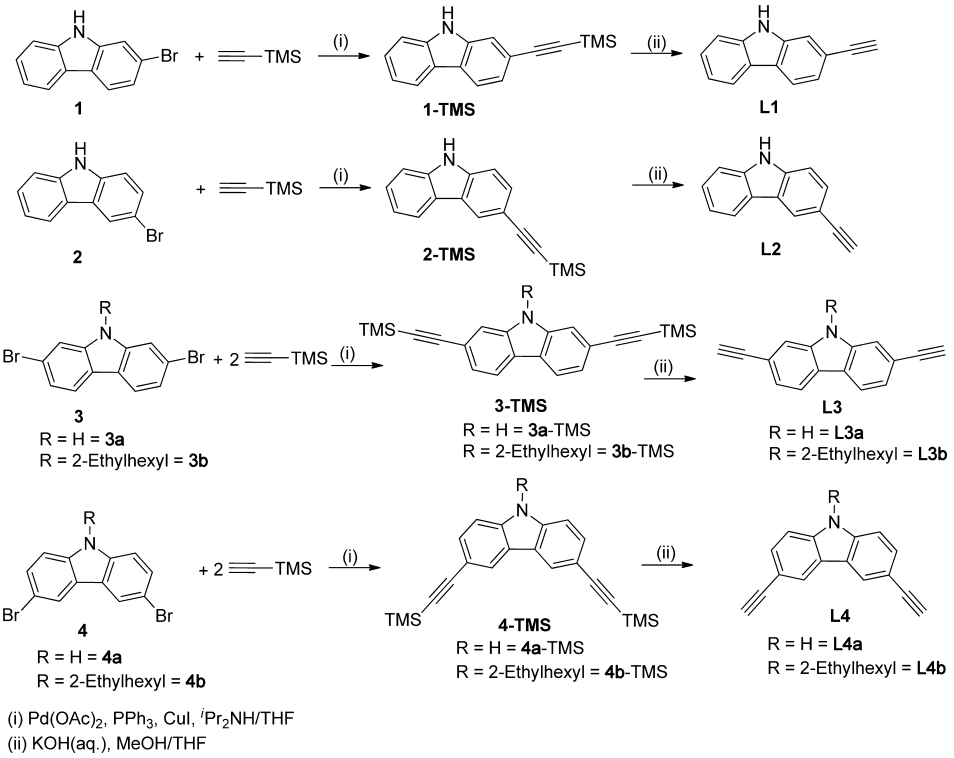

the prospects of both improving polymer processability and mediating potential interchain interactions in polymer films.[8] There is also considerable interest in the solid-state structures of the polymeric materials due to evidence of interchain interactions which influence their optoelectronic properties. In this context, an analysis of intermolecular interactions in the crystal structures of the ligand precursors and of suitable model complexes may lead to a better understanding of the interactions in the polymers.[9] Mono- and diynes are viewed as building blocks for the high molecular-weight poly-ynes, and valuable information on their properties (e.g., electronic structure and optical absorption) can be obtained by studying these model systems. Mono- and diyne compounds are also often more easily crystallized than the corresponding poly-ynes, allowing for a detailed structural analysis and, thus, an assessment of structure−property relationships.[9b]

Several carbazole-based chromophores have been prepared, and their photophysical properties investigated in order to explore their potential applications in organic electroluminescent devices.[10] Several recent reports have also studied the incorporation of carbazole-based auxiliaries into conjugated MOFs.[8b,11] In this work, we report the synthesis and characterization of a set of acetylide-functionalized carbazole ligands and their mono-, di-, and polynuclear Pt(II) σ-acetylide complexes. The crystal structures of two acetylide ligand precursors, together with those of mononuclear and dinuclear Pt(II) σ-acetylide complexes, are also reported. The optoelectronic properties are characterized, compared to those of related organometallic complexes and polymers, and investigated through computational modeling.

RESULTS AND DISCUSSION

Synthesis. Alkylation of 2,7- and 3,6-dibromo carbazoles using NaH in anhydrous DMF was performed in high yields by following the reported literature method.[12] However, the subsequent removal of DMF was found to be a tedious and time-consuming process, which also resulted in significant loss of the final products. Yang et al. alkylated phenothiazine (pKa ~ 23) using potassium *tert*-butoxide (KO^{t}Bu) as the base and THF as the solvent.[13] Since carbazole has a pKa of ~20, we successfully applied Yang's method to alkylate carbazoles. No reaction occurred upon stirring at room temperature for 6−8 h, but refluxing the reaction mixture overnight gave the desired products in quantitative yield (Scheme 1). After completion of the reaction, removal of the solvent *in vacuo*, followed by purification using column chromatography, gave the products in very high yield, making the modified alkylation method more convenient than the existing literature method.[12a]

The mono- and bis-ethynyl carbazole derivatives were synthesized by a sequence of coupling and proto-desilylation reactions (Scheme 2). A total of six trimethylsilyl-protected

DOI: 10.1021/acs.inorgchem.6b00523
Inorg. Chem. XXXX, XXX, XXX−XXX

Scheme 3. Synthesis of the Mono-Nuclear Pt(II) Mono- and Diynes M1−M3, Incorporating Carbazole-2-yl Moiety

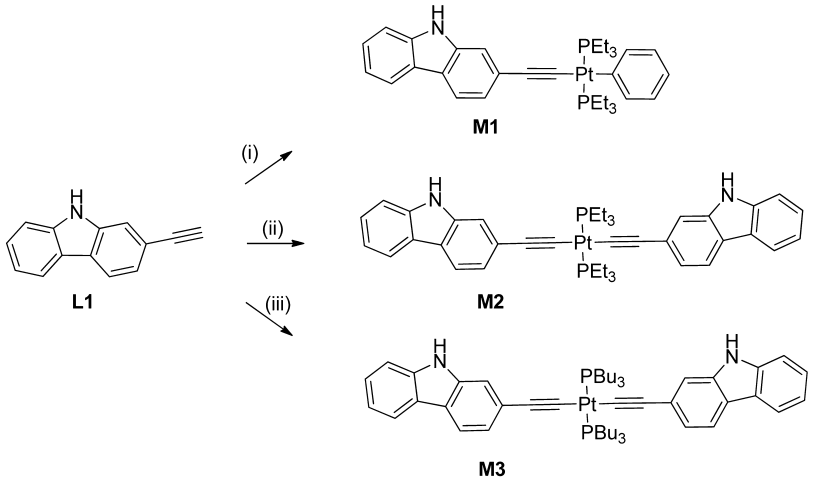

(i) 1.0 equiv. *trans*-[$Ph(PEt_3)_2PtCl$], CuI, $^iPr_2NH$, DCM
(ii) 0.5 equiv. *trans*-[$(PEt_3)_2PtCl_2$], CuI, $^iPr_2NH$, DCM
(iii) 0.5 equiv. *trans*-[$(PBu_3)_2PtCl_2$], CuI, $^iPr_2NH$, DCM

Scheme 4. Synthesis of the Mono-Nuclear Pt(II) Mono- and Diynes M4−M6, Incorporating Carbazole-3-yl Moiety

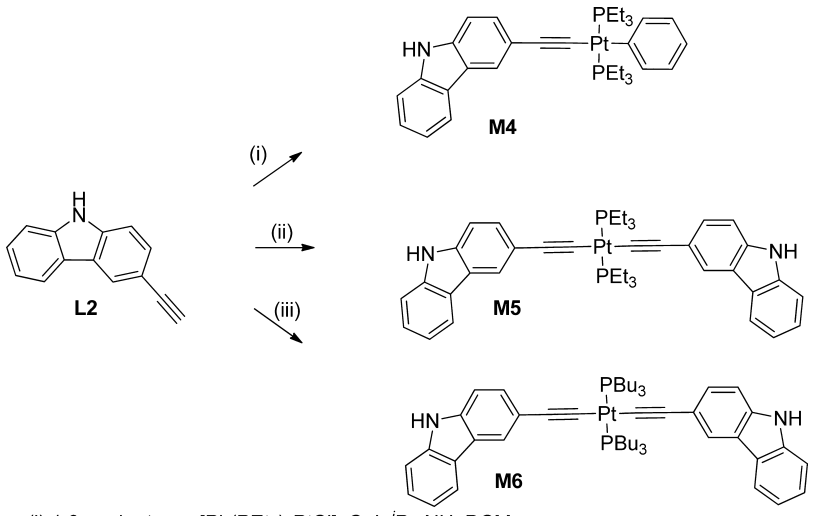

(i) 1.0 equiv. *trans*-[$Ph(PEt_3)_2PtCl$], CuI, $^iPr_2NH$, DCM
(ii) 0.5 equiv. *trans*-[$(PEt_3)_2PtCl_2$], CuI, $^iPr_2NH$, DCM
(iii) 0.5 equiv. *trans*-[$(PBu_3)_2PtCl_2$], CuI, $^iPr_2NH$, DCM

alkynyl ligand precursors were prepared through a scheme adapted from published procedures involving a Pd^{II}/Cu^{I}-catalyzed cross-coupling reaction of the monobromo- or dibromocarbazoles with trimethylsilylethyne in an $^iPr_2NH$/THF solvent:[4c,8b,11,14] 2-trimethylsilylethynylcarbazole (**1-TMS**), 3-trimethylsilylethynylcarbazole (**2-TMS**), 2,7-bis(trimethylsilylethynyl)carbazole (**3a-TMS**), 2,7-bis(trimethylsilylethynyl)-*N*-(2-ethylhexyl)carbazole (**3b-TMS**), 3,6-bis(trimethylsilylethynyl)carbazole (**4a-TMS**), and 3,6-bis(trimethylsilylethynyl)-*N*-(2-ethylhexyl)carbazole (**4b-TMS**). Wong et al. reported that alkylation at the carbazole N atom should precede the cross-coupling reaction with trimethylsilylethyne,[11a] presumably due to the instability of the N−H group in $^iPr_2NH$. However, we were able successfully to introduce trimethylsilylethynyl groups onto the nonalkylated 2,7- and 3,6-carbazoles by conducting the cross-coupling reactions in a mixture of $^iPr_2NH$ and THF.

Conversion of the protected ligand precursors into their terminal alkynes was accomplished by smooth removal of the trimethylsilyl group(s) with dilute aqueous KOH in MeOH/THF, yielding 2-ethynylcarbazole (**L1**), 3-ethynylcarbazole (**L2**), 2,7-bis(ethynyl)carbazole (**L3a**), 2,7-bis(ethynyl)-*N*-(2-ethylhexyl)carbazole (**L3b**), 3,6-bis(ethynyl)carbazole (**L4a**), and 3,6-bis(ethynyl)-*N*-(2-ethylhexyl)carbazole (**L4b**). The products were purified by silica-gel column chromatography and isolated as off-white to light-yellow solids or viscous liquids in 88−99% yields. The trimethylsilyl-protected mono- and bis-alkynes were stable to air and light and were characterized by infrared (IR) spectroscopy, nuclear-magnetic resonance (NMR; ^1H and ^{13}C), electron-impact/electrospray ionization mass spectrometry (EI-MS/ESI-MS), and elemental analyses. The mono- and bis-terminal alkynes were found to be somewhat less stable and hence were freshly prepared before reaction with the Pt(II) bis-phosphine dihalide complexes.

DOI: 10.1021/acs.inorgchem.6b00523
Inorg. Chem. XXXX, XXX, XXX−XXX

Scheme 5. Synthesis of the Di-nuclear Pt(II) Diynes M7 and M8 and the Corresponding Poly-ynes P1 and P2

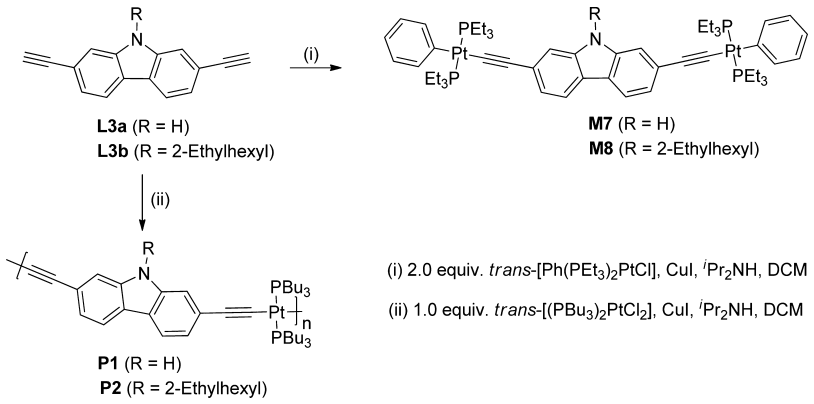

Scheme 6. Synthesis of the Pt(II) Diynes M9 and M10 and the Corresponding Poly-ynes P3 and P4

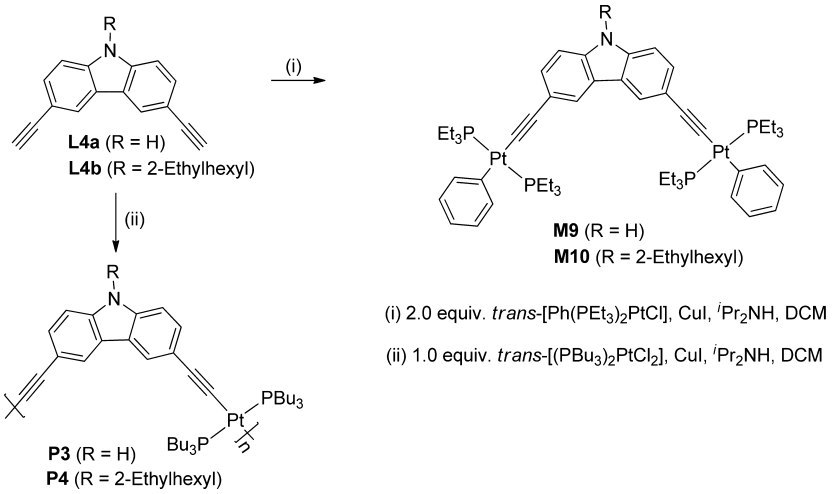

The reaction of the terminal monoalkynes **L1** and **L2** with one equivalent of *trans*-[(Ph)$(Et_3P)_2$PtCl] in $^iPr_2NH/CH_2Cl_2$ in the presence of CuI at room temperature readily afforded the mononuclear Pt(II) monoynes **M1** and **M4**, respectively. Treating **L1** and **L2** with 0.5 equiv of *trans*-[$(Et_3P)_2PtCl_2$] and *trans*-[$(P^nBu_3)_2PtCl_2$] yielded the corresponding mononuclear Pt(II) diynes **M2** and **M5**, and **M3** and **M6**, respectively (Schemes 3 and 4). On the other hand, the reaction of *trans*-[(Ph)$(Et_3P)_2$PtCl] with the terminal dialkynes **L3** and **L4** (1:2 equiv) under similar conditions gave the dinuclear Pt(II) diynes **M7**−**M10** (Schemes 5 and 6). The CuI-catalyzed dehydrohalogenation polycondensation reaction between *trans*-[$(P^nBu_3)_2PtCl_2$] and the terminal dialkynes **L3** and **L4** (1:1 equiv) under similar reaction conditions readily afforded the poly-ynes **P1**−**P4** (Schemes 5 and 6). It is worth noting that ethynylation with Pt(II) chloride complexes proceeded smoothly in basic medium despite the presence of acidic NH protons. We attribute this to the stabilization of carbazole NH protons through H-bonding with solvent as well as other carbazole moiety. The involvement of carbazole NH protons in H-bond possibly prompted the terminal acetylenic protons for the preferential dehydro-halogenation reaction.[15] Purification of the Pt(II) mono- and diynes (**M1**−**M10**) was performed using silica column chromatography, while the Pt(II) poly-ynes (**P1**−**P4**) were purified by chromatography on alumina. The synthesis of the Pt(II) mononuclear diyne **M6**, dinuclear diynes **M7**−**M9**, and poly-ynes **P1**−**P3** were reported previously.[11e,f]

Spectroscopic Characterization. Preliminary characterization of the acetylide-functionalized carbazole ligands and their Pt(II) mono-, di- and poly-ynes was carried out using IR spectroscopy and ^1H, ^{13}C, and ^{31}P NMR. The IR spectra of the Pt(II) mono-, di-, and poly-yne compounds provided clear evidence for the presence of the C≡C bond from its characteristic absorption at around ∼2095 cm^{-1}.[4d,e,8b,11,16] The single, sharp $\nu_{C\equiv C}$ absorptions indicate a *trans*-configuration of the alkynyl bridging ligands around the bis(trialkynylphosphine) Pt(II) moieties. The Pt(II) mono-, di-, and poly-ynes display lower $\nu_{C\equiv C}$ values than those of the terminal alkynes (**L1**−**L4**) which is attributed to metal-to-alkynyl ligand back bonding. The $\nu_{C\equiv C}$ values for the terminal alkynes (**L1**−**L4**; 2104−2108 cm^{-1}) were found to be lower than those of the trimethylsilyl-protected alkynes (**1-TMS**−**4-TMS**; 2148−2152 cm^{-1}); the fact that terminal alkynes (HC≡C−R) have lower $\nu_{C\equiv C}$ frequencies than their protected counterparts RC≡C−R (typically around 50 cm^{-1}) is well-known and thus expected.[17]

The ^1H and ^{13}C NMR spectra of all the compounds contained peaks corresponding to the expected alkyl, aryl, and alkynyl fragments. The peak area ratios in the ^1H NMR spectra were found to agree with the feed mole ratio of the precursors for the mono-, di-, and poly-ynes. The IR and $^{31}P\{^1H\}$-NMR spectral features are similar to those observed in other

DOI: 10.1021/acs.inorgchem.6b00523
Inorg. Chem. XXXX, XXX, XXX−XXX

previously reported Pt(II) mono-, di-, and poly-ynes[18] and indicate an all-*trans* configuration and hence a rigid-rod like structure. The mass-spectrometry results confirm the molecular masses expected for the acetylide ligands and the mono- and dinuclear platinum-acetylide complexes.

Gel-permeation chromatography (GPC), calibrated against a polystyrene standard, gave weight-average molecular weights for the poly-ynes **P1**−**P4** in the range of 17 900−40 500 g/mol, corresponding to degrees of polymerizations (DPs) between 22 and 43. The polydispersity index (PDI) was found to vary between 1.6 and 1.9. These molecular weights should, however, be viewed with caution, due to the difficulties associated with characterizing rigid-rod polymers using GPC. This technique does not give absolute values of the molecular weights, but rather provides a measure of hydrodynamic volume, and rod-like polymers in solution show very different hydrodynamic properties to more flexible polymers. Therefore, calibration of the GPC with a polystyrene standard is likely to artificially increase the measured molecular weights to some extent. However, the lack of discernible resonances corresponding to end groups in the NMR spectra does indicate a high degree of polymerization in these poly-ynes.

Optical-Absorption Spectroscopy. The TMS-protected carbazole ligands, the ten Pt(II) complexes, and the four polymers were found to be readily soluble in common organic solvents, and we therefore measured the room-temperature absorption spectra of all 20 compounds in dilute CH_2Cl_2 solution. Table 1 summarizes absorption spectral data of the compounds. Room-temperature absorption spectra of the 2- and 3-trimethylsilylacetylide carbazole ligands (**1-TMS** and **2-TMS**) and corresponding mononuclear Pt(II) complexes (**M1**−**M3** and **M4**−**M6**, respectively) are shown in Figure 1.

Table 1. Optical Absorption Data for Protected Ligands and Pt(II) Complexes Incorporating Carbazole Spacers[a]

compound	$\lambda_{max,1}$	ε_1	λ_{2max}	ε_2	λ_{3max}	ε_3
1-TMS	258	1.60	315	1.57		
2-TMS	246	1.25	280	1.63		
3a-TMS	253	1.71	325	1.25		
3b-TMS	265	1.50	269	1.47	335	1.60
4a-TMS	257	1.78	290	1.73		
4b-TMS	261	1.69	297	1.74		
M1	242	1.36	350	1.50		
M2	242	1.85	354	1.67		
M3	243	1.65	357	1.78		
M4	241	1.73	290	1.14	325	0.83
M5	242	1.73	292	1.21	342	0.87
M6	242	1.80	291	1.42	340	1.15
M7	250	1.89	354	0.51		
M8	266	1.39	373	1.62		
M9	291	1.68	315	1.48	323	0.52
M10	244	1.83	318	0.94	328	0.83
P1	262	1.47	323	0.54	352	0.46
P2	265	1.75	400	1.48		
P3	264	2.62	293	1.60	335	0.47
P4	257	1.95	350	1.78		

[a]Absorption spectra were taken in CH_2Cl_2 at room temperature ($\varepsilon \times 10^{-5}/M^{-1}cm^{-1}$, λ_{max}/nm).

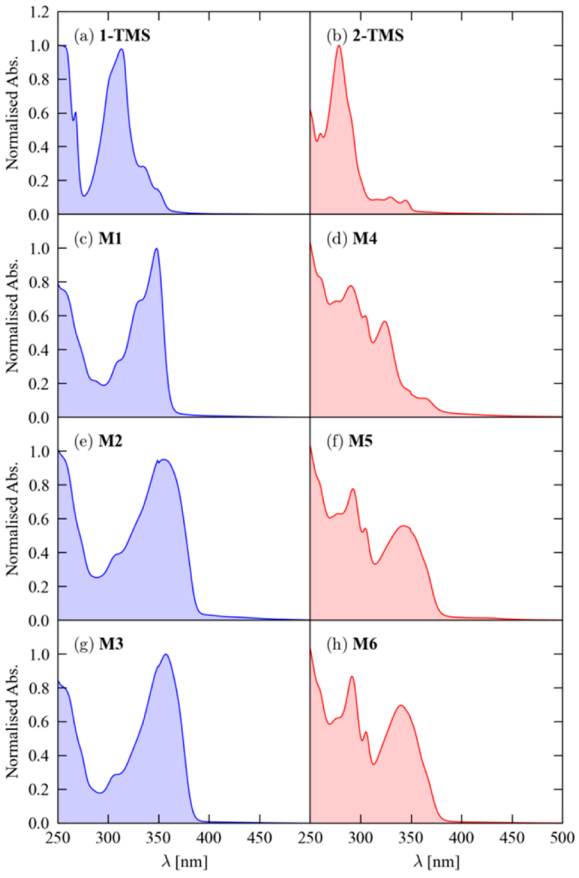

Figure 1. Solution absorption spectra (CH_2Cl_2) of the 2- and 3-trimethylsilylacetylide carbazole ligands **1-TMS** (a) and **2-TMS** (b), together with those of the corresponding mononuclear Pt(II) complexes **M1**−**M3** (c, e, g) and **M4**−**M6** (d, f, h).

The spectrum of **1-TMS** displays a pair of strong absorption bands at 258 and 315 nm, which overlap to form an asymmetric peak, and two weaker shoulder features at ∼340 and 350 nm. In contrast, **M1** displays an intense, narrow absorption band at 350 nm, with higher-energy shoulders at 330 and 310 nm. The spectra of **M2** and **M3** are similar in form, with both displaying broad, asymmetric peaks with maxima around 360 nm; this shape might be likened to the spectrum of **M1**, but with the lower-energy transitions broadened and slightly red-shifted. The spectrum of **M2** displays a noticeable shift in the absorption edge with respect to **M1** and **M3**, although the low-energy absorptions in all three complexes are significantly enhanced with respect to **1-TMS**. This points toward extended delocalization in the complexes, across the Pt(II) center and between the aromatic ligands; the red shift seen in the absorption edge of **M2** and **M3** compared to **M1** may be explained by the higher degree of electronic delocalization possible over the two carbazole ligands in these complexes, versus the single carbazole ligand and phenyl ring in **M1**.

In contrast, the spectrum of **2-TMS** has a sharp maximum and shoulder feature at ∼280 and 290 nm, respectively, with some fine structure at longer wavelengths including two comparatively much weaker peaks around 335 and 350 nm. The considerable blue shift compared to the 2-carbazole acetylide analogue is mirrored in the spectra of the Pt(II) complexes **M4**−**M6**. As with **M1**−**M3**, complexation leads to an enhancement of the lower-energy absorption features, with the spectrum of **M4** displaying sharper features than those of **M5** and **M6**. The first absorption band in the spectrum of **M4** occurs around 370 nm but is considerably weaker than the clear peak ∼325 nm. As for **M2** and **M3**, the spectra of **M5** and **M6**

DOI: 10.1021/acs.inorgchem.6b00523
Inorg. Chem. XXXX, XXX, XXX−XXX

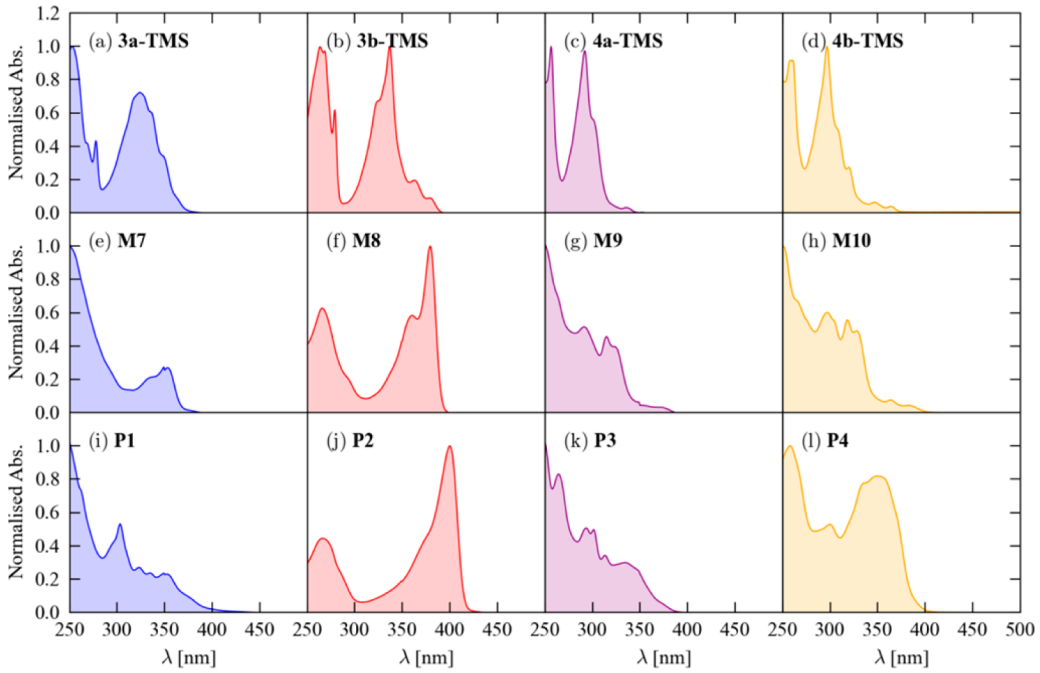

Figure 2. Solution absorption spectra (CH_2Cl_2) of the 2,7- and 3,6-functionalized TMS-protected carbazole ligands **3a**/**3b-TMS** (a, b) and **4a**/**4b-TMS** (c, d) and the corresponding dinucelar Pt(II) complexes **M7**−**M10** (e−h) and polymers **P1**−**P4** (i−l).

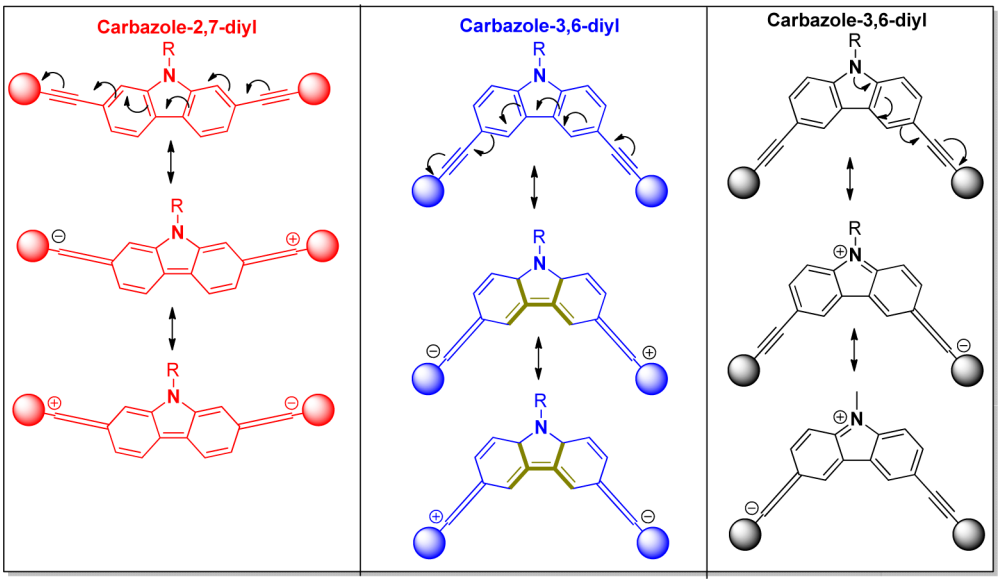

Figure 3. Schematic illustration of the electronic delocalization across the carbazole-2,7-diyl and carbazole-3,6-diyl spacers. Adapted with permission from ref 11f. Copyright 2006 AIP Publishing LLC.

consist of broad low-energy absorption peaks but with the maxima blue-shifted to 340−350 nm. However, the absorption edge of both 3-carbazole complexes is noticeably broader than that of the 2-carbazole analogues. We also recorded and compared room-temperature absorption spectra of the 2,7- and 3,6-functionalized TMS-protected carbazole ligands (**3a**/**3b-TMS** and **4a**/**4b-TMS**, respectively) and the corresponding dinuclear Pt(II) complexes (**M7**−**M10**) and polymers (**P1**−**P4**) (Figure 2).

Comparing Figure 2a,b and c,d, the changes to the spectra on alkylating the N atom are subtle but noticeable. The first absorption maximum of **3a-TMS** occurs at ∼325 nm, with shoulder features at 335−340 and approximately 350 nm, while the maximum of **3b-TMS** was measured at 335 nm, and the shoulder features at ∼360 and 380 nm. The spectrum of the alkylated 2,7-acetylide carbazole also has sharper features than the H form, particularly in the low-energy part of the spectrum, although this difference is not apparent for the 3,6-functionalized carbazoles. **4a-TMS** has an absorption maximum at ∼290 nm, a shoulder around 300 nm, and a weaker absorption at approximately 340 nm, whereas in the alkylated **4b-TMS** the maximum and shoulders occur at 295−300 and 310/320 nm, with a pair of smaller peaks at 350 and 365 nm. For both the 2,7- and 3,6-carbazole systems, alkylation thus leads to a slight enhancement of the long-wavelength part of the absorption spectrum. The spectroscopy suggests that alkylation induces a

DOI: 10.1021/acs.inorgchem.6b00523
Inorg. Chem. XXXX, XXX, XXX−XXX

small red shift in the absorption, although this is secondary to the significant blue shift observed between the 2,7- and 3,6-substitution patterns; the latter is analogous to the blue shift between the 2- and 3-functionalized carbazoles evident in Figure 1 and can be understood qualitatively as a loss in electronic delocalization in the 3,6-substituted ligand (Figure 3), which possesses a so-called "break junction" in the molecular structure. As per the figure, complete delocalization across the 3,6-diyl spacer is not possible without generating pentavalent carbon centers (Figure 3, middle), which is not possible. Another possibility of delocalization is involving the lone pair on the nitrogen atom, leading to the generation of charged centers. Overall, delocalization was favored in the case of 2,7-isomers, while it is less in 3,6-diyl-isomers.

The photophysical properties of **M7**−**M9** and **P1**−**P3** in the solid state have been previously reported,[11f] and we observed no significant differences in the band shapes and absorption maxima in thin films and solution, except for some very small shifts in band positions, which can be attributed to the differences in environment. As for the mononuclear complexes, incorporation of the ligands into dinuclear Pt(II) complexes lead to a red shift in the absorption edge. In contrast, however, the clear trend of an enhancement of the low-energy absorption is less clear-cut for **M7**−**M10**. There is a sharp increase in intensity of the absorption edge of **M8**, whereas there seems to be a reduction in the intensity of the long-wavelength part of the spectrum of **M7**, although this is relative to the bright band at ∼250 nm and not on an absolute scale. With reference to the spectra of the protected carbazole ligands, the spectra of **M9** and **M10** appear to show a broadening of the sharp features in the spectra of **4a-** and **4b-TMS**, respectively, in addition to the apparent red shift in the feature positions. Compared to the dinuclear complexes **M7**−**M10**, the polymers **P1**−**P4** show a further red shift in the absorption, consistent with the extended electronic delocalization, together with a general broadening of the spectral features. The polymers also show a relative increase in long-wavelength absorption, which is particularly noticeable in the cases of **P2** and **P4**.

To summarize, from the spectroscopic characterization, we extract four general observations:

(1) The 3- and 3,6-substituted carbazoles and their complexes display a blue-shifted absorption compared to the 2- and 2,7-substituted analogues, which may be attributed to a reduction in electronic delocalization in the former ligands due to the presence of a break junction.
(2) Incorporation of the carbazole spacers into Pt(II) complexes generally leads to an enhancement of the absorption in the longer-wavelength part of the profile.
(3) Functionalization of the carbazole N atom can in principle allow the absorption profile to be tuned.
(4) The polymers show a further red shift and a broadening of the absorption profiles with respect to the model dinuclear complexes.

Extended conjugation across the metal centers in these complexes is consistent with previous results on related systems,[10a,11a,14,19] and the red shifts in the spectra of the complexes and polymers compared to those of the protected ligands, suggestive of electronic excitations between highly delocalized states, is consistent with observations made from other Pt(II) poly-ynes incorporating carbocyclic and heterocyclic spacers.[3a,14,16a]

Crystal Structures. In order to complement the spectroscopic characterization of the polymer precursors, we attempted to grow single crystals suitable for X-ray diffraction of several of the key precursors and intermediates in the synthesis. We were able to obtain suitable single crystals of the 2,7- and 3,6-carbazole trimethylsilyl-acetylide ligands (**3a-TMS**, **4a-TMS**) and of the mono- and dinuclear Pt(II) σ-acetylide compounds **M3** and **M7**, and thus, crystallographic studies were carried out on these systems. The structures of **3a-TMS**, **4a-TMS**, and the model compounds **M3** and **M7** are shown in Figures 4−8, and key crystallographic parameters are summarized in Table 2.

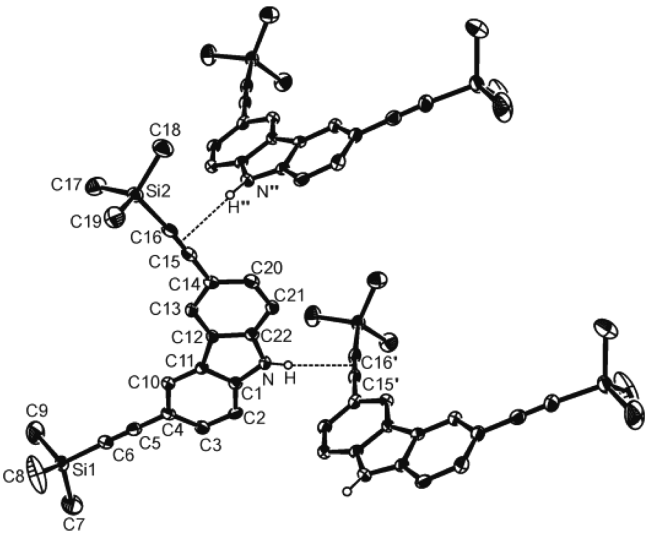

Figure 4. Structure of **4a-TMS** showing the atom-numbering scheme; thermal ellipsoids are set at 40% probability.

Molecules of **4a-TMS** (Figure 4), which lack *N* functionalization but have the 3,6-alkynyl substitution pattern, aggregate through a hydrogen bond between the N−H group and the midpoint of the C(15)≡C(16) bond of a neighboring molecule [N−H···midpoint distance 2.392 Å; N−H−midpoint angle 162.90°]. However, this has no significant impact on the length of the alkyne bond [1.208(5) Å] in comparison to that of the nonhydrogen bonded group [C(5)≡C(6); 1.202(4) Å]. In contrast, the structure of **3a-TMS** (Figure 5), which has the alkynyl groups at the 2,7 positions, has too much steric crowding around the N−H to allow for this interaction. All the intramolecular bond lengths and angles for both **3a-TMS** and **4a-TMS** lie within the expected ranges.

The molecular structure of the mononuclear Pt(II) diyne **M3** is illustrated in Figure 6. The molecule occupies a crystallographic center of symmetry, which is coincident with the central platinum atom. This metal exhibits the *trans*-square planar geometry suggested by the spectroscopic characterization, which is consistent with that found in the related platinum poly-yne molecules.[4e,8b] The platinum−alkynyl σ-interaction has a Pt(1)−C(3) distance of 2.002(2) Å, which is within the expected range. The ethynylenic unit is almost linear [∠Pt(1)−C(3)−C(4) 175.7(2)°, ∠C(3)−C(4)−C(5) 172.3(3)°], and the C(3)−C(4) bond is similar, at 1.210(3) Å, to that observed in the precursor **3a-TMS**. The carbazolyl unit is essentially planar (maximum deviation from the C(5)−N(17) unit of −0.038 Å for C(5); RMSD 0.019 Å), and the bond parameters are not significantly different to those

DOI: 10.1021/acs.inorgchem.6b00523
Inorg. Chem. XXXX, XXX, XXX−XXX

Table 2. Crystallographic Data for 3a-TMS, 4a-TMS, M3, and M7

	3a-TMS	4a-TMS	M3	M7
CCDC deposition no.	1 456 923	14 569 324	14 569 325	1 456 926
empirical formula	$C_{22}H_{25}NSi_2$	$C_{22}H_{25}NSi_2$	$C_{52}H_{70}N_2P_2Pt$	$C_{53}H_{81}NOP_4Pt_2$
molecular weight	359.61	359.61	980.13	1262.2
T/K	150(2)	150(2)	100(2)	150(2)
crystal system	monoclinic	orthorhombic	triclinic	monoclinic
space group	$P2_1$	$P2_12_12_1$	P-1	$P2_1/n$
a/Å	6.1804(2)	6.3292(2)	9.5643(3)	21.0064(3)
b/Å	10.9724(4)	7.7163(3)	10.5536(4)	8.3268(1)
c/Å	16.4113(5)	43.8439(17)	11.9787(4)	30.8889(4)
α/°	90	90.00	78.149(3)	90.00
β/°	90.271(2)	90.00	81.742(3)	92.058(1)
γ/°	90	90.00	78.372(3)	90
V/Å^3	112.90(6)	2141.25(14)	1152.43(7)	5399.48(12)
Z	2	4	1	4
ρ/g cm^{-3}	1.073	1.116	1.412	1.553
μ/mm^{-1}	0.163	0.170	3.150	5.33
F(000)	384	768	504	2520
crystal size/mm	0.60 × 0.60 × 0.10	0.50 × 0.40 × 0.01	0.30 × 0.15 × 0.10	0.30 × 0.30 × 0.05
radiation	Mo Kα (λ = 0.71073 Å)	Mo Kα (λ = 0.71073 Å)	Mo Kα (λ = 0.71073 Å)	Mo Kα (λ = 0.71073 Å)
2θ range for data collection/°	3.53 to 37.95	5.58 to 52.74	6.44 to 59.16	3.579 to 25.348
index ranges	$-7 \le h \le 7$, $-13 \le k \le 13$, $-19 \le l \le 19$	$-7 \le h \le 7$, $-9 \le k \le 9$, $-54 \le l \le 54$	$-13 \le h \le 13$, $-14 \le k \le 14$, $-16 \le l \le 16$	$-25 \le h \le 25$, $-9 \le k \le 10$, $-37 \le l \le 37$
reflections collected	12 451	35 204	14 717	18 102
independent reflections	3795 [R_{int} = 0.0928]	4375 [R_{int}= 0.0745]	5584 [R_{int}= 0.0473]	9838 [R_{int} = 0.0586]
data/restraints/parameters	3795/2/236	4375/0/236	5584/37/263	9839/533/628
goodness-of-fit on F^2	1.160	1.135	0.956	1.052
final R indexes [$I \ge 2\sigma(I)$]	R_1 = 0.0559, wR_2 = 0.1297	R_1 = 0.0674, wR_2 = 0.1514	R_1 = 0.0314, wR_2 = 0.0420	R_1 = 0.0529, wR_2 = 0.1086
final R indexes [all data]	R_1 = 0.0602, wR_2 = 0.1313	R_1 = 0.0736, wR_2 = 0.1546	R_1 = 0.0329, wR_2 = 0.0424	R_1 = 0.0883, wR_2 = 0.1189
largest diff. peak/hole/e Å^{-3}	0.299/−0.187	0.61/−0.39	1.23/−0.79	1.298/−0.954
absolute structure parameter	−0.20 (15)			

DOI: 10.1021/acs.inorgchem.6b00523
Inorg. Chem. XXXX, XXX, XXX−XXX

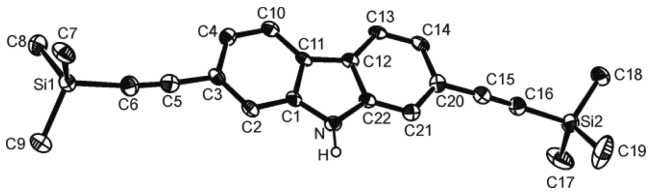

Figure 5. Structure of **3a-TMS** showing the atom-numbering scheme; thermal ellipsoids are set at 40% probability.

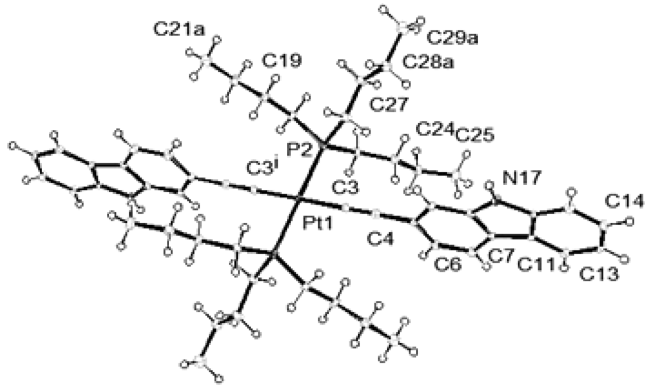

Figure 6. Structure of **M3** showing the atom-numbering scheme; thermal ellipsoids are set at 40% probability. Selected geometric data (distances in Å, angles in °): Pt(1)−C(3) 2.002(2), Pt(1)−P(2) 2.3200(6), C(3)−C(4) 1.210(3), ∠Pt(1)−C(3)−C(4) 175.7(2), and ∠C(3)−Pt(1)−P(2) 91.61(7).

observed in **3a-TMS**, the diyne **M7** (Figure 7), and in other, related, reported carbazole structures.[11a,e] The carbazolyl ring plane makes an angle of 81.88° with the square planar Pt unit (Pt(1), P(2), C(3), P(2i), C(3i)); the "i" atoms are related to those in the asymmetric unit by the symmetry operation (−*x*, −*y*, −*z*).

M7 crystallizes as a methanol solvate [PhPt(PEt_3)$_2$C≡CC≡C(PEt_3)$_2$PtPh]·MeOH, with one molecule each of the complex and solvent in the asymmetric unit (Figure 7). The methanolic oxygen atom acts as a hydrogen-bond acceptor[20] to the carbazole N−H group [H(1)···(1) 2.02 Å, N(1)···O(1) 2.869(10) Å, ∠N(1)−H(1)···O(1) 161.9°]. The methanolic hydrogen atom acts as a hydrogen-bond donor to the C≡C C(19)−C(20) on an adjacent molecule (Figure 8), though again this has no significant influence on the length of the C≡C bond [1.212(12) Å] which, as in the structure of **4a-TMS**, is not significantly different from the length of the other alkyne bond [C(33)≡C(34); 1.208(13) Å]. The two Pt(II) centers adopt the expected square planar geometry, as observed in a wide variety of diplatinum diyne complexes with a range of central spacer groups.[4d,e,8b,11a−d,16] The dihedral angle between the two platinum-containing planes is 35.5°. The terminal phenyl rings on each platinum are planar and essentially perpendicular to the Pt-coordination planes; the angle between the planes containing the atoms Pt(1)P(1)P(2)C(13)C(19) and the C(13)−C(18) ring is 84.5° and that between the planes containing the atoms Pt(2)P(3)P(4)C(34)C(35) and C(35)−C(40) is 90.0°. The acetylenic units show only slight deviations from linearity, with ∠Pt(1)−C(19)−C(20) 175.3(8)°, ∠Pt(2)−C(34)−C(33) 171.6(12)°, ∠C(19)−C(20)−C(21) 177.1(10)°, and ∠C(31)−C(33)−C(34) 171.0(13)°. The central carbazole group is essentially planar, with angles of 2.2° and 1.3° between the C(21)−C(26) and N(1)C(24)C(25)C(27)C(28) planes and between the N(1)-C(24)C(25)C(27)C(28) and C(24)C(27)C(29)C(30)C(31)-C(32) planes, respectively. The interplanar angle between Pt(1)P(1)P(2)C(13)C(19) and C(21)−C(26) is 45.7° and that between the Pt(2)P(3)P(4)C(34)C(35) and C(24)C(27)-C(29)C(30)C(31)C(32) planes is 82.9°.

The Pt−P distances average 2.286 Å, and the Pt−C(≡C) bond lengths average 2.01 Å, which is slightly shorter than the average Pt−C(Ph) bond length of 2.03 Å. These values are consistent with the geometries of related diplatinum diynes.[4d,e,8b,11a−d,16] The two acetylenic C≡C bond lengths average 1.21 Å, which is, again, within the expected range. The bond parameters within the carbazole spacer group do not show any significant deviations from those reported in 3-(trimethylsilylethynyl)carbazole[20] and are consistent with those in the mononuclear platinum complex *trans-bis*(carbazol-3-ylethynyl)*bis*-tri-*n*-butylphosphine-platinum(II).[11e]

Across all four structures, the C_{10}−C_{11}, C_{11}−C_{12}, and C_{12}−C_{13} bond distances in the heterocycle (numbering as in Chart 1), and the bond lengths in the C−C≡C groups, are the same within experimental error. Thus, the proposed enhanced delocalization within the carbazole-2,7-diyl derivatives compared to the 3,6-substituted analogues (Figure 3) appears to have no discernible effect on the bond lengths. The data are also consistent with previously reported structures of Pt, Au, and Hg complexes of carbazole-3,6-diyls.[8b]

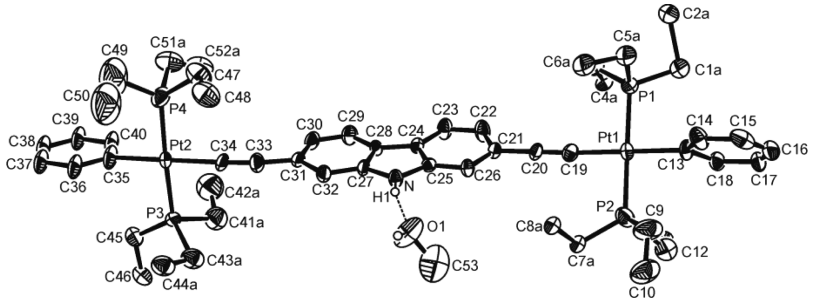

Figure 7. Structure of **M7** showing the atom-numbering scheme and the interaction with the methanol solvent molecule. Only one orientation of the disordered component of the structure (labeled Ca) is shown for clarity; C(3a) and C(11) are obscured by C(6a) and C(12), respectively. Thermal ellipsoids are set to 40% probability. Selected geometric data (distances in Å, angles in °): Pt(1)−P(1) 2.294(3), Pt(1)−P(2) 2.277(3), Pt(2)−P(3) 2.282(3), Pt(2)−P(4) 2.291(3), Pt(1)−C(13) 2.064(9), Pt(1)−C(19) 2.007(9), Pt(2)−C(35) 2.072(3), Pt(1)−C(34) 2.013(9), C(19)−C(20) 1.212(12), C(33)−C(34) 1.208(13), ∠Pt(1)−C(19)−C(20) 175.3(8), ∠Pt(2)−C(34)−C(33) 171.6(12), ∠C(19)−C(20)−C(21) 177.1(10), and ∠C(31)−C(33)−C(34) 171.0(13).

DOI: 10.1021/acs.inorgchem.6b00523
Inorg. Chem. XXXX, XXX, XXX−XXX

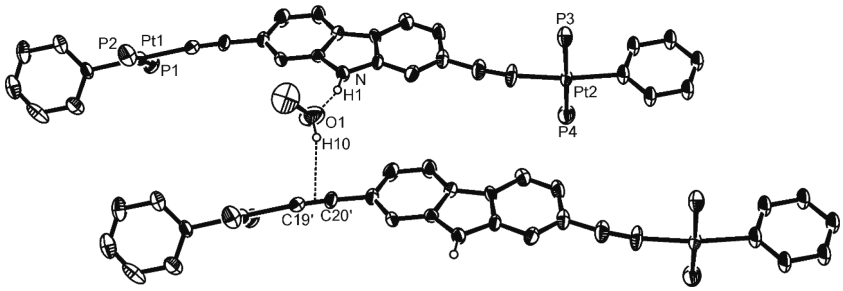

Figure 8. Association of the **M7** diyne molecules through solvent-mediated hydrogen bonding. Selected geometric data (distances in Å, angles in °): N−H(1)···O(1) 2.02, ∠N−H(1)···O(1) 161.7, O−H···midpoint C(19′)−C(20′) 2.31, and ∠O−H···midpoint C(19′)−C(20′) 157.0.

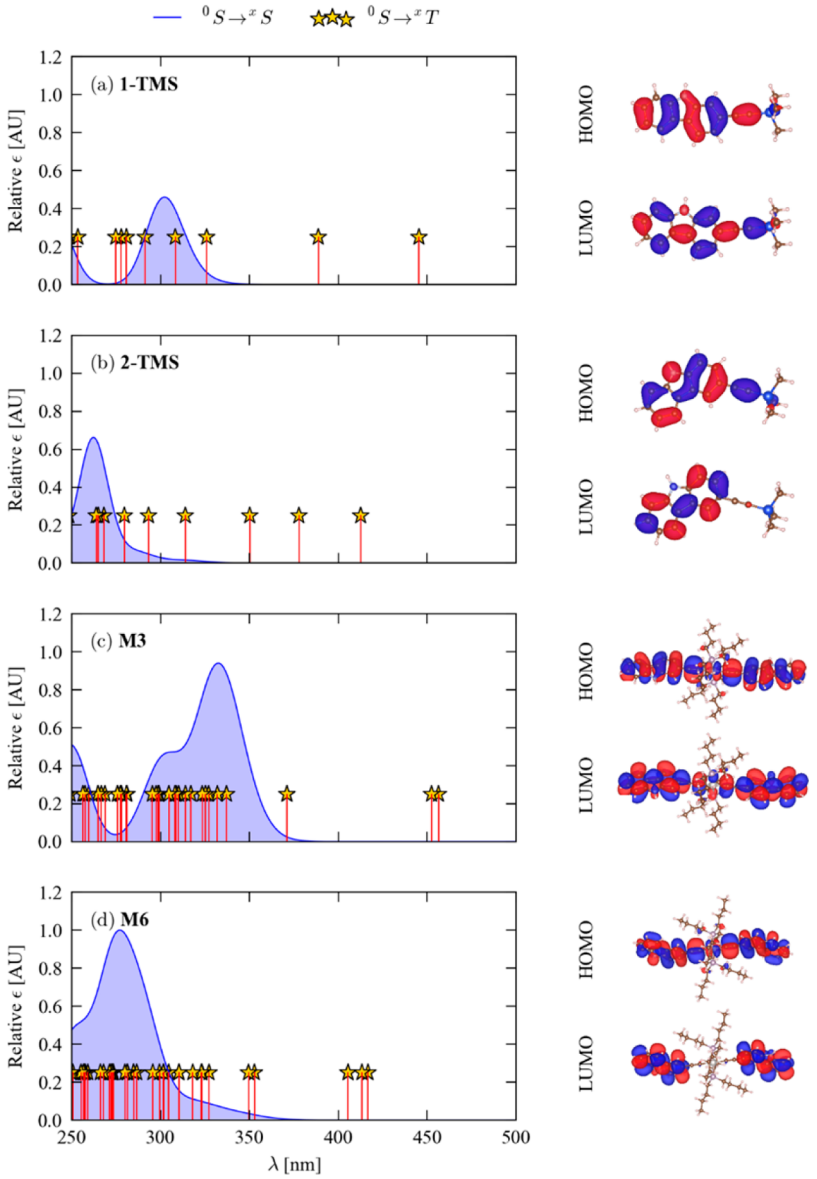

Figure 9. Simulated gas-phase absorption spectra of **1-TMS** (a), **2-TMS** (b), **M3** (c), and **M6** (d) from time-dependent density-functional theory (TD-DFT) using adiabatic B3LYP.[21] Each plot shows the simulated absorption profile obtained from the spin-allowed (singlet) states (blue), with the spin-forbidden (triplet) states marked by red lines/gold stars. Isosurface plots of the highest-occupied and lowest-unoccupied molecular orbitals (HOMOs/LUMOs) for each system are shown to the right of the simulated spectra. These plots were prepared using the VESTA software.[22]

Computational Modeling. To complement the optical spectroscopy and in particular to understand the origin of the spectral changes observed between the carbazole ligands with different substitution patterns and the Pt(II) complexes, we performed gas-phase molecular quantum-chemical calculations on **1-TMS**, **2-TMS**, **M3**, and **M6**.[11e] The four models were optimized at the hybrid density-functional theory (DFT) level of theory, and the minima were verified by computing

DOI: 10.1021/acs.inorgchem.6b00523
Inorg. Chem. XXXX, XXX, XXX−XXX

Table 3. HOMO−LUMO Gaps ($E_{H\text{-}L}$) and Energies, Wavelengths, Oscillator Strengths (f), and Assignments of the "Brightest" Low-Energy Transitions (λ > 300 nm) in Gas Phase 1-TMS, 2-TMS, M3, and M6, Obtained from Time-Dependent Density-Functional Theory (TD-DFT) Using Adiabatic B3LYP[21,a]

model	$E_{H\text{-}L}$/eV	E/eV	λ/nm	f	assignment
1-TMS	4.417	3.860	302.3	0.757	HOMO → LUMO (85.3%)
2-TMS	4.579	3.945	313.6	0.024	HOMO → LUMO (87.6%)
					HOMO − 1 → LUMO + 1 (10.5%)
M3	4.085	3.720	333.3	1.471	HOMO → LUMO (92.9%)
M6	4.085	3.877	319.9	0.137	HOMO → LUMO + 2 (80.5%)
					HOMO → LUMO + 3 (17.5%)

[a]The assignments are based on the percentage of the sum of the squared coefficients (given in brackets), and only the major components of the overall transition are listed.

vibrational frequencies. We then performed time-dependent DFT (TD-DFT) calculations on these optimized models to investigate the optical properties and to characterize the electronic excitations. The computational methodology is described in detail in the Experimental Section.

Figure 9 shows the simulated absorption spectra of the four complexes, together with isosurface plots of the frontier highest-occupied and lowest-unoccupied molecular orbitals (HOMOs/LUMOs). The simulated spectra compare reasonably well with the corresponding solution spectra in Figure 1 and in particular mirror the key trends observed from these measurements, viz., the red shift and stronger absorption of the 2-substituted carbazoles and their Pt(II) complexes compared to the 3-substituted analogues and also of both Pt(II) complexes compared to the TMS-protected ligands.

Aside from some small shifts in the positions of absorption bands, a notable discrepancy between the simulated and experimentally recorded spectra is the presence of additional fine structure (e.g., shoulders) in the latter. Two possible reasons for this are that (1) a constant peak broadening was assumed when generating the simulated spectra (see Experimental Section), whereas in general each state may have a different line width, and (2) low-energy singlet excitations with small oscillator strengths, of which there are several in the **M3** and **M6** Pt(II) complexes, could be enhanced relative to the brighter transitions at finite temperature by geometric distortions induced through thermal vibration. Furthermore, as evident in Figure 9, all four complexes possess low-lying triplet excitations; these are formally spin forbidden but in principle could also contribute to small features in the spectra.

To interpret the spectroscopic activity of the four complexes, we chose to analyze the "brightest" low-energy transition in each, i.e., the excitations with the highest oscillator strengths, f, among the transitions with excitation wavelengths above 300 nm. Table 3 lists the excitation energies/wavelengths, oscillator strengths, and an assignment of each state in terms of contributions from individual orbital transitions; the calculated HOMO−LUMO gap is also given for reference.

In **1-TMS**, there are two predicted transitions with λ > 300 nm. The brightest of these, at 302 nm, can be assigned as a HOMO−LUMO excitation, although there is a considerably weaker transition between the HOMO − 1 and LUMO orbitals at 321 nm (f = 0.032). Mirroring the blue shift observed experimentally, **2-TMS** has a single, comparatively weak calculated transition above 300 nm (λ = 314 nm, f = 0.024), which can be assigned to the HOMO → LUMO absorption with a small contribution from the HOMO − 1 → LUMO + 1 excitation. From inspection of the frontier orbitals, it is apparent that both the HOMO and LUMO in **1-TMS** are more delocalized than the corresponding orbitals in **2-TMS**, which could account for the smaller energy gap and longer excitation wavelengths of **1-TMS**.

As can be seen clearly from the data in Table 3, incorporation of the carbazole ligands into Pt(II) complexes leads to a red shift in the absorption energies and a substantial enhancement of the oscillator strengths, which once again mirrors the observations made from the spectroscopy. The very strong low-energy absorption at 333 nm in **M3** is due to the HOMO−LUMO transition, and from inspection of the orbitals, the red shift can be explained by delocalization of the HOMO orbitals in the two carbazole ligands across the metal center. A similar pattern is observed in **M6**, for which the composite HOMO → LUMO and HOMO −1 → LUMO − 1 transition in **2-TMS** undergoes a red shift and an increase in oscillator strength (λ = 343 nm, f = 0.054). However, in this complex, there is also a considerably brighter transition at 320 nm, corresponding to a redistribution of electron density from the HOMO to the LUMO + 2 and LUMO + 3 orbitals, and it is this excitation which makes the largest contribution to the long-wavelength tail feature in the simulated spectrum. The oscillator strength of this transition, however, is still an order of magnitude smaller than the HOMO−LUMO transition in **M3**. In summary, the computational modeling presented here confirms the key inferences drawn from the optical spectroscopy and confirms (1) that the frontier orbitals in the 2-substituted carbazole ligands are more delocalized than those in the 3-substituted analogues and (2) that the red shift and enhancement of the absorption in the Pt(II) complexes can be explained by delocalization of the ligand HOMO orbitals across the Pt centers.

CONCLUSION

We have synthesized and characterized a series of acetylide-functionalized carbazole ligands and Pt(II) mono-, di-, and poly-ynes incorporating 2-, 3-, 3,6-, and 2,7-carbazole spacer groups. We have reported crystal structures of several of these precursors and model compounds, providing insight into possible intermolecular interactions in the polymeric systems, viz., hydrogen bonding between the carbazole N−H and alkyne groups on neighboring molecules, which may be mediated by included solvent molecules. This study has also shed valuable light on the relationship between molecular and electronic structure in this family of systems, in particular showing that there is a significantly higher degree of electronic delocalization within the complexes and polymers with the 2- and 2,7-functionalized ligands compared to those with the 3- and 3,6-substituted ones, which leads to a marked red shift in the absorption spectra. Incorporation of the carbazole ligands into

DOI: 10.1021/acs.inorgchem.6b00523
Inorg. Chem. XXXX, XXX, XXX−XXX

Pt(II) complexes produces a further red shift and an enhancement of the low-energy absorption profile, which can be explained by electronic delocalization between ligands across the Pt(II) centers. These hypotheses have been confirmed both spectroscopically and using computational modeling. Organometallic rigid-rod polymers based on carbazole-2,7-diyl units are expected to display enhanced electron transport within the chains, whereas polymers based on the carbazole-3,6-diyl analogue are expected to show poorer transport properties. The systematic study carried out in this work should assist in the future rational design of conjugated Pt(II) poly-ynes with improved optoelectronic properties for a range of technological applications.

EXPERIMENTAL SECTION

General Procedures. All reactions were performed under a dry Ar atmosphere using the standard Schlenk technique. Solvents were predried and distilled before use according to standard procedures.[23] All chemicals, except where stated otherwise, were obtained from Sigma-Aldrich and used as received. The compounds **3a**,[24] *trans*-[(Ph)(PEt$_3$)$_2$PtCl],[25] and *trans*-[(P^{n}Bu$_3$)$_2$PtCl$_2$][26] were prepared according to literature procedures. NMR spectra were recorded in $CDCl_3$ using Bruker WM-250 and AM-400 spectrometers and a Bruker Avance III HD 700 MHz spectrometer equipped with 5 mm TCI H/C/N cryoprobe. The ^{1}H and ^{13}C{^{1}H} NMR spectra were referenced to solvent resonances, and the ^{31}P{^{1}H}NMR spectra were referenced to external trimethylphosphite or 85% H_3PO_4. IR spectra were recorded either in CH_2Cl_2 solutions in a NaCl cell using a PerkinElmer 1710 FT-IR spectrometer or directly on the sample as attenuated total reflectance (ATR) on Diamond using a Cary 630 FT-IR spectrometer. UV/vis spectra were recorded with Shimadzu UV-2450 spectrometer. Mass spectra were acquired using a Kratos MS 890 spectrometer using electron-impact (EI) and electrospray-ionization (ESI) techniques. Microanalyses were carried out at the University Chemical Laboratory, University of Cambridge. Preparative thin-layer chromatography was carried out on commercial Merck plates with a 0.25 mm layer of silica. Column chromatography was performed using either Kieselgel 60 silica gel (230−400 mesh) or Brockman grade II−III alumina.

Caution! *All chemicals used in the current work are sensitive to skin, eyes, and the respiratory system. Therefore, all reactions were performed in a well-ventilated fume hood. Inhalation of silica/alumina and low boiling solvents like dichloromethane and hexane may cause injuries to internal organs. Safety glasses, gloves, masks, and lab coats were worn during the experiments.*

Ligand Synthesis. *2,7-Dibromo-N-(2-ethylhexyl)carbazole,* ***3b.*** A mixture of 2,7-carbazole **3a** (1.00 g, 3.08 mmol) and potassium *tert*-butoxide (KO^{t}Bu) (0.415 g, 3.70 mmol) in dry THF (80 mL) was placed in a two-necked flask and stirred at room temperature for 20 min under an Ar atmosphere. 2-Ethylhexyl bromide (0.640 mL, 3.70 mmol) was added to the reaction mixture, which was then refluxed overnight. After removing the solvent, the crude product was purified using a silica-gel column eluted with hexane, yielding a white solid (1.32 g, 97.8%). ^{1}H NMR (700 MHz, $CDCl_3$, ppm) δ 7.89 (d, J = 8.2 Hz, 2H, H-4, 5), 7.34 (dd, J = 8.2, 1.2 Hz, 2H, H-3, 6), 7.26 (s, 2H, H-1,8), 4.07 (d, J = 8.0 Hz, 2H, N−CH_2), 2.02 (hept, J = 6.7 Hz, 1H, alkyl CH), 1.45−1.22 (m, 8H, alkyl CH_2), 0.89 (ddt, J = 31.4, 24.3, 12.3 Hz, 6H, alkyl CH_3). ^{13}C NMR (176 MHz, $CDCl_3$, ppm) δ 141.86, 122.53, 121.43, 121.25, 119.66, 112.31 (aromatic), 47.70 (N−CH_2), 41.06 (alkyl CH), 31.90, 29.72, 28.56, 24.34 (alkyl CH_2), 14.08, 10.91 (alkyl CH_3). ESI-MS: m/z 437.21 (M^+). Anal. Calc. for $C_{20}H_{23}Br_2N$: C, 54.94; H, 5.30. Observed: C, 55.01; H, 5.32%.

3,6-Dibromo-N-(2-ethylhexyl)carbazole, ***4b.*** The same procedure as used to synthesize **3b** using 3,6-dibromocarbazole **4a** was followed. The product was obtained as a colorless viscous liquid (96.2%). ^{1}H NMR (700 MHz, $CDCl_3$, ppm) δ 7.90 (s, 2H, H-4, 5), 7.39 (dd, J = 8.7, 1.8 Hz, 2H, H-1, 8), 7.06 (d, J = 8.7 Hz, 2H, H-2, 7), 3.92−3.82 (m, 2H, N−CH_2), 1.87−1.77 (m, 1H, alkyl CH), 1.26−1.06 (m, 8H, alkyl CH_2), 0.81−0.67 (m, 6H, alkyl CH_3). ^{13}C NMR (176 MHz, $CDCl_3$, ppm) δ 162.56, 139.61, 129.09, 123.61, 123.33, 112.20, 110.87 (aromatic), 47.55 (N−CH_2), 39.41 (alkyl CH), 32.15, 30.88, 28.64, 24.25 (alkyl CH_2), 13.73, 10.66 (alkyl CH_3). ESI-MS: m/z 437.15 (M^+). Anal. Calc. for $C_{20}H_{23}Br_2N$: C, 54.94; H, 5.30. Observed: C, 55.02; H, 5.31%.

2-(Trimethylsilyl)-9H-carbazole, ***1-TMS.*** To a solution of 2-bromocarbazole **1** (1.00 g, 4.06 mmol) in ^{i}Pr$_2$NH/THF (70 mL, 1:4 v/v) under an Ar atmosphere were added catalytic amounts of CuI (10 mg), $Pd(OAc)_2$ (10 mg), and PPh_3 (52 mg). The solution was stirred for 30 min at room temperature, and then trimethylsilylethyne (0.87 mL, 6.09 mmol) was added under vigorous stirring. The reaction mixture was then refluxed overnight. The completion of the reaction was confirmed by silica TLC and IR spectroscopy. After being cooled to room temperature, the mixture was filtered and concentrated *in vacuo*. The impure residue was redissolved in CH_2Cl_2 and purified by silica column chromatography using a hexane/CH_2Cl_2 (1:1 v/v) eluent to yield a pale yellow solid (0.85 g, 79%, mp 218 °C). IR (ATR, diamond): ν/cm^{-1} 3402 (N−H), 2151 (−C≡C−). ^{1}H NMR (700 MHz, $CDCl_3$, ppm): δ, 8.04 (d, J = 8.1 Hz, 2H, H-4, 5), 7.99 (d, J = 8.0 Hz, 1H, H-8), 7.55 (s, 1H, H-1), 7.43 (m, 2H, H-6, 7), 7.35 (d, J = 8.0 Hz, 1H, H-3), 5.76 (s, 1H, NH), 0.28 (s, 9H, $SiMe_3$). ^{13}C NMR (176 MHz, $CDCl_3$, ppm): δ 140.24, 139.03, 132.27, 126.55, 123.76, 123.10, 120.71, 120.25, 120.14, 119.94, 114.32, 110.85 (aromatic), 106.39, 93.70 (−C≡C−), 0.22 ($SiMe_3$). ESI-MS: m/z 261.9 (M^+). Anal. Calc. for $C_{17}H_{17}NSi$: C, 77.52; H, 6.51. Observed: C, 77.55; H, 6.53%.

3-(Trimethylsilyl)-9H-carbazole, ***2-TMS.*** A similar procedure to that used for the synthesis of **1-TMS** was adopted using 3-bromocarbazole **2**. The compound was obtained as a white solid (0.79 g, 73%, mp 189 °C). IR (ATR, diamond): ν/cm^{-1} 3392 (N−H), 2148 (−C≡C−). ^{1}H NMR (700 MHz, $CDCl_3$, ppm): δ 8.22 (s, 1H, H-4), 8.11 (br s, 1H, NH), 8.04 (d, J = 7.8 Hz, 1H, H-5), 7.53 (d, J = 8.3 Hz, 1H, H-8), 7.48−7.39 (m, 3H, H-2, 6, 7), 7.33 (d, J = 8.3 Hz, 1H, H-1), 0.29 (s, 9H, $SiMe_3$). ^{13}C NMR (176 MHz, $CDCl_3$, ppm): δ 139.89, 139.35, 129.97, 126.47, 124.67, 123.36, 123.05, 120.62, 120.11, 114.00, 110.88, 110.60 (aromatic), 106.65, 91.91 (−C≡C−), 0.31 ($SiMe_3$). ESI-MS: m/z 261.9 (M^+). Anal. Calc. for $C_{17}H_{17}NSi$ C, 77.52; H, 6.51. Observed: C, 77.60; H, 6.50%.

2,7-Bis(trimethylsilylethynyl)carbazole, ***3a-TMS.*** A similar procedure to that used for the synthesis of **1-TMS** was adopted using 3,6-dibromocarbazole **3** (1.20 g, 3.69 mmol), CuI (7 mg), $Pd(OAc)_2$ (8 mg), PPh_3 (48 mg), and trimethylsilylethyne (1.30 mL, 9.22 mmol). The product was isolated as a pale brown solid (1.2 g, 90%, mp 184.7−185.2 °C). IR (CH_2Cl_2): ν/cm^{-1} 3401 (N−H), 2150 (−C≡C−). ^{1}H NMR (700 MHz, $CDCl_3$, ppm): δ 8.06 (br s, 1H, NH), 7.95 (d, J = 8.1 Hz, 2H, H-4, 5), 7.58 (s, 2H, H-1, 8), 7.54 (d, J = 8.3 Hz, 2H, H-3, 6), 0.28 (s, 18H, $SiMe_3$). ^{13}C NMR (176 MHz, $CDCl_3$, ppm): δ 140.81, 139.51, 124.10, 123.92, 123.10, 122.95, 121.67, 120.57, 120.31, 120.09, 114.29, 113.80 (aromatic), 105.99, 95.04 (−C≡C−), 0.03 ($SiMe_3$). ESI-MS: m/z 359.6 (M^+). Anal. Calc. for $C_{22}H_{25}Si_2N$: C, 73.50; H, 7.01. Observed: C, 73.74; H, 7.02%.

3,6-Bis(trimethylsilylethynyl)carbazole, ***4a-TMS.*** A similar procedure to that used for the synthesis of **1-TMS** was adopted using 3,6-dibromocarbazole **4a** and afforded a pale yellow solid (60.1%). IR (CH_2Cl_2): ν/cm^{-1} 3394 (N−H), 2149 (−C≡C−). ^{1}H NMR (700 MHz, $CDCl_3$,): δ 8.32 (br s, 1H, NH), 8.18 (s, 2H, H-4, 5), 7.54 (dd, J = 8.3, 1.1 Hz, 2H, H-1, 8), 7.33 (d, J = 8.3 Hz, 2H, H-2, 7), 0.29 (s, 18H, $SiMe_3$). ^{13}C NMR (176 MHz, $CDCl_3$) δ 139.61, 130.40, 124.84, 122.96, 114.65, 110.78 (aromatic), 106.32, 92.31 (−C≡C−), 0.33, 0.32, 0.32, 0.30, 0.16, 0.14 ($SiMe_3$). ESI-MS: m/z 359.5 (M^+). Anal. Calc. for $C_{22}H_{25}NSi_2$: C, 73.51; H, 7.01. Observed: C, 73.66; H, 7.08%.

2,7-Bis(trimethylsilylethynyl)-N-(2-ethylhexyl)carbazole, ***3b-TMS.*** A similar procedure to that followed in the synthesis of **1-TMS** was adopted using **3b** and afforded a pale yellow solid (71%). IR (CH_2Cl_2): ν/cm^{-1} 2151 (−C≡C−). ^{1}H NMR (700 MHz, $CDCl_3$, ppm): δ 7.96 (d, J = 8.0 Hz, 2H, H-4, 5), 7.47 (s, 2H, H-1, 8), 7.33 (dd, J = 8.0, 1.0 Hz, 2H, H-3, 6), 4.12 (ddd, J = 36.3, 14.8, 7.6 Hz, 2H, N−CH_2), 2.12−2.01 (m, 1H, alkyl CH), 1.44−1.22 (m, 8H, alkyl CH_2), 0.92−0.82 (m, 6H, alkyl CH_3), 0.33−0.24 (m, 18H, $SiMe_3$). ^{13}C

DOI: 10.1021/acs.inorgchem.6b00523
Inorg. Chem. XXXX, XXX, XXX−XXX

NMR (176 MHz, $CDCl_3$): δ 140.97, 123.18, 122.54, 120.22, 120.19, 112.64 (aromatic), 106.35, 93.75 (−C≡C−), 47.51 (N−CH_2), 39.09 (alkyl CH), 30.70, 28.49, 24.37, 23.00 (alkyl CH_2), 14.00, 10.92 (alkyl CH_3), 0.03, 0.01 ($SiMe_3$). ESI-MS: m/z 472.0 (M^+). Anal. Calc. for $C_{30}H_{41}Si_2N$: C, 76.39; H, 8.76. Observed: C, 76.45; H, 8.75%.

3,6-Bis(trimethylsilylethynyl)-N-(2-ethylhexyl)carbazole, ***4b-TMS.*** A similar procedure to that used in the synthesis of **1-TMS** was followed using **4b** and afforded a pale yellow viscous liquid (80%). IR (CH_2Cl_2): ν/cm^{-1} 2152 (−C≡C−). ^{1}H NMR (700 MHz, $CDCl_3$, ppm): δ 8.19 (s, 2H, H-4, 5), 7.56 (dd, J = 8.4, 1.5 Hz, 2H, H-1, 8), 7.28 (dd, J = 8.3, 3.8 Hz, 2H, H-2, 7), 4.12 (d, J = 7.6 Hz, 2H, N−CH_2), 2.00 (hep, J = 6.8 Hz, 1H, alkyl CH), 1.39−1.14 (m, 8H, alkyl CH_2), 0.89 (t, J = 7.4 Hz, 3H, alkyl CH_3), 0.82 (t, J = 7.2 Hz, 3H, alkyl CH_3), 0.31−0.14 (m, 18H, $SiMe_3$). ^{13}C NMR (176 MHz, $CDCl_3$, ppm): δ 141.05, 129.85, 124.79, 122.70, 113.82, 109.24 (aromatic), 106.50, 92.29 (−C≡C−), 47.66 (N−CH_2), 39.32 (alkyl CH), 30.60, 28.87, 24.17, 23.06 (alkyl CH_2), 14.13, 10.91 (alkyl CH_3), 0.28, 0.28, 0.25, 0.19, 0.16, 0.12 ($SiMe_3$). ESI-MS: m/z 472.0 (M^+). Anal. Calc. for $C_{30}H_{41}Si_2N$: C, 76.39; H, 8.76. Observed: C, 76.45; H, 8.75%.

2-(Ethynyl)-9H-carbazole, ***L1.*** **1-TMS** (0.600 g, 2.28 mmol) was proto-desilylated in THF/methanol (20 mL, 4:1, v/v) using aqueous KOH (0.19 g, 3.45 mmol). The reaction mixture was stirred at room temperature for 1 h, during which time TLC and IR revealed that all the protected compounds had been converted to the terminal alkyne ligand. The solvent was then removed, and the residue was dissolved in CH_2Cl_2 and purified by column chromatography on silica using hexane/CH_2Cl_2 (1:1, v/v) as eluent, to give the product as a pale brown solid (0.391 g, 89.8%). IR (ATR, diamond): ν/cm^{-1} 2104 (−C≡C−), 3276 (C≡C−H). ^{1}H NMR (250 MHz, $CDCl_3$, ppm): δ 9.11 (s, 1H, NH), 7.56 (s, 1H, H-1), 7.54 (d, J = 7.9 Hz, 1H, H-8), 7.51 (d, J = 8.1 Hz, 1H, H-4), 7.40 (d, J = 7.9 Hz, 1H, H-5), 7.16 (d, J = 7.4 Hz, 1H, H-3), 7.08−7.00 (m, 2H, H-6, 7), 3.06 (s, 1H, C≡C−H). ^{13}C NMR (100 MHz, $CDCl_3$, ppm): δ 135.52, 133.43, 131.14, 126.05, 125.63, 124.10, 123.22, 121.98, 120.15, 118.52, 114.31, 112.53 (aromatic), 105.9, 82.4 (−C≡C−). ESI-MS m/z 191.99 (M^+). Anal. Calc. for $C_{14}H_9N$: C, 87.93; H, 4.74. Observed: C, 88.01; H, 4.73%.

3-(Ethynyl)-9H-carbazole, ***L2.*** A similar procedure to the one followed for the synthesis of **L1** was adopted using **2-TMS** and afforded a pale yellow solid (87.6%). IR (ATR, diamond): ν/cm^{-1} 2108 (−C≡C−), 3300 (C≡C−H). ^{1}H NMR (250 MHz, $CDCl_3$, ppm): δ 9.93 (s, 1H, NH), 7.70 (d, J = 7.7 Hz, 1H, H-1), 7. 55 (d, J = 7.8 Hz, 1H, H-8), 7.50 (d, J = 8.0 Hz, 1H, H-4), 7.40 (d, J = 8.2 Hz, 1H, H-5), 7.24 (d, J = 7.7 Hz, 1H, H-2), 7.08 (t, J = 7.2 Hz, 1H, H-7), 7.00 (t, J = 7.4 Hz, 1H, H-6), 3.06 (s, 1H, C≡C−H). ^{13}C NMR (100.6 MHz, $CDCl_3$, ppm): δ 138.43, 134.25, 132.15, 131.17, 127.46, 125.11, 123.26, 123.01, 122.36, 120.06, 116.10, 113.46 (aromatic), 107.3, 105.9 (−C≡C−). ESI-MS: m/z 192.2 (M^+). Anal. Calc. for $C_{14}H_9N$: C, 87.93; H, 4.74. Observed: C, 87.98; H, 4.72%.

2,7-Bis(ethynyl)carbazole, ***L3a.*** A similar procedure to that used to synthesize **L1** was adopted using **3a-TMS** and afforded a pale brown solid (93.0%). IR (CH_2Cl_2): ν/cm^{-1} 2105 (−C≡C−), 3302 (C≡C−H). ^{1}H NMR (700 MHz, $CDCl_3$, ppm) δ 8.12 (br s, 1H), 7.88 (d, J = 8.3 Hz, 2H, H-4, 5), 7.58 (s, 2H, H-1, 8), 7.36 (d, J = 8.2 Hz, 2H, H-3, 6), 3.14 (s, 2H, C≡C−H). ^{13}C NMR (176 MHz, $CDCl_3$, ppm) δ 140.15, 138.81, 125.39, 123.90, 122.93, 121.78, 120.23, 119.50, 114.57, 113.68, 110.62, 109.26 (aromatic), 86.75, 84.29 (−C≡C−). ESI-MS: m/z 216.1 (M^+). Anal. Calc. for $C_{16}H_9N$: C, 89.28; H, 4.19. Observed: C, 89.70; H, 4.26%.

2,7-Bis(ethynyl)-N-(2-ethylhexyl)carbazole, ***L3b.*** A similar procedure to that followed to synthesize **L1** was adopted using **3b-TMS** and afforded the product as a pale yellow viscous liquid (98.7%). IR (CH_2Cl_2): ν/cm^{-1} 2105 (−C≡C−), 3298 (C≡C−H). ^{1}H NMR (700 MHz, $CDCl_3$, ppm) δ 8.00 (d, J = 8.0 Hz, 2H, H-4, 5), 7.53 (s, 2H, H-1, 8), 7.37 (d, J = 8.0 Hz, 2H, H-3, 6), 4.13 (qd, J = 14.8, 7.7 Hz, 2H, N−CH_2), 3.16 (s, 2H, C≡C−H), 2.06 (m, 1H, alkyl-CH), 1.44−1.22 (m, 8H, alkyl CH_2), 0.94−0.83 (m, 6H, alkyl CH_3). ^{13}C NMR (176 MHz, $CDCl_3$, ppm) δ 141.03, 123.24, 122.81, 120.49, 119.33, 113.06 (aromatic), 84.90 (−C≡C−), 47.64 (N−CH_2), 39.26 (alkyl CH), 30.87, 28.64, 24.37, 23.06 (alkyl CH_2), 14.02, 10.92 (alkyl CH_3). ESI-MS: m/z 328.2 (M^+). Anal. Calc. for $C_{24}H_{25}N$: C, 88.03; H, 7.70. Observed: C, 88.14; H, 7.65%.

3,6-Bis(ethynyl)carbazole, ***L4a.*** A similar procedure as was used to synthesize **L1** was followed using **4a-TMS** and afforded the product as a colorless microcrystalline solid (98.3%). IR (CH_2Cl_2): ν/cm^{-1} 2105 (−C≡C−), 3302 (C≡C−H). ^{1}H NMR (700 MHz, $CDCl_3$, ppm) δ 8.20 (s, 1H, NH), 8.13 (s, 2H, H-4, 5), 7.57 (d, J = 8.3 Hz, 2H, H-1, 8), 7.36 (d, J = 8.3 Hz, 2H, H-2, 7), 3.07 (s, 2H, CC−H). ^{13}C NMR (176 MHz, $CDCl_3$, ppm) δ 139.73, 138.55, 130.41, 129.27, 124.89, 124.00, 123.25, 122.40, 113.57, 112.96, 112.22, 110.88 (aromatic), 84.40, 84.04 (−C≡C−). ESI-MS: m/z 216.3 (M^+). Anal. Calc. for $C_{16}H_9$ N: C, 89.28; H, 4.19. Observed: C, 89.48; H, 4.21%.

3,6-Bis(ethynyl)-N-(2-ethylhexyl)carbazole, ***L4b.*** A similar procedure to that used in the synthesis of **L1** was followed using **4b-TMS** and afforded the product as a yellow viscous liquid (90.0%). IR (CH_2Cl_2): ν/cm^{-1} 2104 (−C≡C−), 3299 (C≡C−H). ^{1}H NMR (250 MHz, $CDCl_3$, ppm): δ 7.99 (d, J = 7.6 Hz, 2H, H-4, 5), 7.51 (s, 2H, H-1, 8), 7.36 (dd, J = 13.8, 7.3 Hz, 2H, H-3, 6), 4.10−4.12 (m, 2H, N−CH_2), 3.15 (s, 2H, C≡C−H), 2.05−2.08 (m, 1H, alkyl CH), 1.25−1.29 (m, 8H, alkyl CH_2), 0.87−0.88 (m, 6H, alkyl CH_3). ^{13}C NMR (100.6 MHz, $CDCl_3$, ppm): δ 142.53, 137.63, 132.49, 130.10, 123.22, 122.83, 120.95, 120.02, 119.46, 117.46, 113.01, 112.31 (aromatic), 106.56, 89.91 (−C≡C−), 48.10 (N−CH_2), 40.32 (CH), 30.95, 28.62, 24.41, 22.94 (alkyl CH_2), 14.97, 11.24 (alkyl CH_3). ESI-MS: m/z 327.97 (M^+). Anal. Calc. for $C_{24}H_{25}N$: C, 88.03; H, 7.70. Observed: C, 88.14; H, 7.65%.

Synthesis of Pt(II) Mono-, Di-, and Poly-ynes. *trans-[R−C≡C−(PEt$_3$)$_2$Pt−Ph] (R = Carbazole-2-yl),* ***M1.*** To a stirred mixture of **L1** (0.100 g, 0.522 mmol) and *trans*-[Ph(PEt$_3$)$_2$PtCl] (0.284 g, 0.522 mmol) in ^{i}Pr$_2$NH (20 mL) and CH_2Cl_2 (20 mL) was added CuI (1 mg). The solution was stirred at room temperature under Ar over a period of 18 h, after which all volatile components were removed under vacuum. The crude product was taken up in CH_2Cl_2 and passed through a silica column with hexane/CH_2Cl_2 (1:1, v/v) as eluent. The product was obtained as a pale brown solid (0.300 g, 82.6%, mp 170.2 °C). IR (ATR, diamond): ν/cm^{-1} 3230.9 (N−H), 2079 (−C≡C−). ^{1}H NMR (700 MHz, $CDCl_3$, ppm): δ, 7.99 (d, J = 7.7 Hz, 1H, H-5), 7.92 (s, 1H, H-1), 7.88 (d, J = 8.0 Hz, 1H, H-4), 7.40−7.31 (m, 3H, H-8 and H$_{ortho}$ of Ph), 7.20 (dd, J = 13.8, 7.3 Hz, 1H, H-3), 6.97 (t, J = 7.1 Hz, 1H, H$_{para}$ of Ph), 6.90 (dt, J = 24.4, 7.1 Hz, 2H, H$_{meta}$ of Ph), 6.81 (t, J = 7.1 Hz, 2H, H-6, 7), 5.29 (br s, 1H, NH), 1.92−1.33 (m, 12H, PCH_2), 1.14−0.94 (m, 18H, alkyl CH_3). ^{13}C NMR (176 MHz, $CDCl_3$, ppm): δ 139.90, 139.87, 139.37, 136.94, 128.02, 127.45, 127.20, 125.24, 123.84, 123.48, 122.04, 121.36, 120.74, 120.08, 119.78, 119.46, 113.17, 113.09 (aromatic), 111.26, 110.49 (−C≡C−), 15.43−13.56 (PCH_2), 8.27−7.86 (alkyl CH_3). ^{31}P{^{1}H}NMR (122 MHz, DMSO-d_6, ppm): δ 11.46, $^1J_{Pt-P}$ = 2631.5 Hz. ESI-MS: m/z 696.9 (M^+). Anal. Calc. for $C_{34}H_{43}NP_2Pt$: C, 63.72; H, 7.20. Observed: C, 63.80; H, 7.22%.

trans-[R−C≡C−(PEt$_3$)$_2$Pt−C≡C−R] (R = Carbazole-2-yl), ***M2.*** A similar procedure as was used in the synthesis of **M1** was followed using **L1** (0.100 g, 0.522 mmol) and *trans*-[Pt(PEt$_3$)$_2$Cl$_2$] (0.132 g, 0.261 mmol) and CuI (1 mg). The monomer was obtained as a pale brown solid (0.326 g, 77.3%, mp 280.4 °C). IR (ATR, diamond): ν/cm^{-1} 3395 (N−H), 2092 (−C≡C−). ^{1}H NMR (700 MHz, $CDCl_3$, ppm): 8.00 (d, J = 7.5 Hz, 2H, H-5, 5′), 7.95 (s, 2H, H-1, 1′), 7.90 (d, J = 7.7 Hz, 2H, H-4, 4′), 7.43 (dd, J = 14.6, 8.1 Hz, 2H, H-8, 8′), 7.20 (t, J = 7.4 Hz, 4H, H-6, 6′,7, 7′), 7.14 (d, J = 8.0 Hz, 2H, H-3, 3′), 5.28 (s, 2H, NH, NH′), 1.31−1.25 (m, 12H, PCH_2), 1.16−1.08 (m, 18H, CH_3). ^{13}C NMR (176 MHz, $CDCl_3$, ppm): δ 139.94, 139.75, 136.13, 134.25, 129.84, 127.66, 125.56, 125.42, 123.71, 123.38, 123.25, 121.30, 120.19, 120.16, 119.90, 119.86, 119.54, 112.67 (aromatic), 110.56, 110.54 (−C≡C−), 18.35−14.72 (PCH_2), 8.60−8.13 (alkyl CH_3). ^{31}P{^{1}H}NMR (122 MHz, $CDCl_3$, ppm): δ 11.98, $^1J_{Pt-P}$ = 2769.4 Hz. ESI-MS: m/z 810.3 (M^+). Anal. Calc. for $C_{40}H_{46}N_2P_2Pt$: C, 59.18; H, 5.71. Observed: C, 59.23; H, 5.73%.

trans-[R−C≡C-(Bu$_3$P)$_2$Pt−C≡C−R] (R = Carbazole-2-yl), ***M3.*** A similar procedure as was used in the synthesis of **M1** was followed using **L1** (0.100 g, 0.522 mmol), *trans*-[(PBu$_3$)$_2$PtCl$_2$] (0.175 g, 0.261 mmol), and CuI (1 mg). The product was obtained as a biege powder

DOI: 10.1021/acs.inorgchem.6b00523
Inorg. Chem. XXXX, XXX, XXX−XXX

(0.224 g, 87.5%, mp 242.6 °C). IR (ATR, diamond): ν/cm^{-1} 3383 (N−H), 2084 (−C≡C−). ^{1}H NMR (700 MHz, $CDCl_3$, ppm): δ, 8.00 (d, J = 7.7 Hz, 2H, H-4, 4′), 7.94 (s, 2H, H-1, 1′), 7.89 (d, J = 8.0 Hz, 2H, H-5, 5′), 7.39 (d, J = 7.9 Hz, 2H, H-8, 8′), 7.35 (dd, J = 15.1, 7.2 Hz, 2H, H-3, 3′), 7.19 (t, J = 8.1 Hz 4H, 6, 6′,7, 7′), 5.29 (br s, 2H, NH, NH′), 1.72−1.42 (m, 36H, alkyl CH_2), 0.94 (m, 18H, alkyl CH_3). ^{13}C NMR (176 MHz, $CDCl_3$, ppm): δ 139.80, 139.76, 126.88, 125.33, 123.77, 123.42, 120.88, 120.09, 119.76, 119.81, 112.80, 110.50 (aromatic), 110.08, 108.19, 108.11, 108.03 (−C≡C−), 26.56−24.01 (alkyl CH_2), 14.01−13.86 (alkyl CH_3). ^{31}P{^{1}H}-NMR (122 MHz, $CDCl_3$, ppm): δ 4.04, $^1J_{Pt-P}$ = 2368.0 Hz. ESI-MS: m/z 980.3 (M^+). Anal. Calc. for $C_{52}H_{70}N_2P_2Pt$: C, 63.72; H, 7.20. Observed: C, 63.90; H, 7.21%.

trans-[R−C≡C−(PEt$_3$)$_2$Pt−Ph] (R = Carbazole-3-yl), ***M4.*** A similar procedure to that used to synthesize **M1** was followed using **L2** and afforded a pale brown solid (76.6%, mp 154.1 °C). IR (ATR, diamond): ν/cm^{-1} 3406 (N−H), 2085 (−C≡C−). ^{1}H NMR (700 MHz, $CDCl_3$, ppm): δ 8.04 (d, J = 7.7 Hz, 1H, H-5), 8.00 (s, 1H, H-4), 7.97 (s, 1H, NH), 7.41−7.37 (m, 2H, H_{ortho} of Ph), 7.20 (dd, J = 9.1, 4.5 Hz, 2H, H-1, 8), 6.97 (t, J = 7.1 Hz, 3H, H_{para}, H_{meta} of Ph), 6.93 (d, J = 6.0 Hz, 1H, H-2), 6.81 (t, J = 7.0 Hz, 2H, H-7, 6), 1.40 (m, 12H, PCH_2), 0.90 (m, 18H, alkyl CH_3). ^{13}C NMR (176 MHz, $CDCl_3$, ppm): δ 1156.88, 139.93, 139.44, 137.38, 129.61, 128.00, 127.65, 127.38, 125.95, 125.72, 123.47, 123.39, 122.44, 121.25, 120.93, 120.46, 119.55, 119.33 (aromatic), 110.71, 110.65, 110.20, 109.31 (−C≡C−), 15.43−13.45 (PCH_2), 8.28−7.85 (alkyl CH_3). ^{31}P{^{1}H}NMR (122 MHz, $CDCl_3$, ppm): δ 10.73, $^1J_{Pt-P}$ = 2653.5 Hz. ESI-MS: m/z 698.0 (M^+). Anal. Calc. for $C_{34}H_{43}NP_2Pt$: C, 63.72; H, 7.20. Observed: C, 63.81; H, 7.22%.

trans-[R−C≡C−(PEt$_3$)$_2$Pt−C≡C−R] (R = Carbazole-3-yl), ***M5.*** A similar procedure to the synthesis of **M2** using **L2** afforded a pale yelllow solid (69.2%, mp 209 °C). IR (ATR, diamond): ν/cm^{-1} 3387 (N−H), 2096 (−C≡C−). ^{1}H NMR (700 MHz, $CDCl_3$, ppm): δ 8.03 (s, 2H, H-4, 4′), 7.81 (d, J = 7.6 Hz, 2H, H-5, 5′), 7.56−7.51 (m, 4H, H-1, 1′,8, 8′), 7.37 (d, J = 7.9 Hz, 2H, H-2, 2′), 7.16−7.11 (m, 4H, H-6, 6′,7, 7′), 5.22 (s, 2H, NH, NH′), 1.25−1.11 (m, 12H, PCH_2), 0.83−0.73 (m, 18H, alkyl CH_3). ^{13}C NMR (176 MHz, $CDCl_3$, ppm): δ 139.96, 137.72, 137.57, 136.23, 134.52, 134.38, 134.33, 134.29, 134.25, 134.04, 130.30, 130.05, 129.84, 129.54, 129.39, 127.89, 127.82, 127.66, 125.97, 125.83, 123.43, 123.28, 122.54, 120.47, 119.57, 119.45 (aromatic), 110.70, 110.68, 110.35, 110.26 (−C≡C−), 14.75−14.65 (PCH_2), 8.64−8.26 (alkyl CH_3). ^{31}P{^{1}H}NMR (122 MHz, $CDCl_3$, ppm): δ 11.89, $^1J_{Pt-P}$ = 2104.1 Hz. ESI-MS: m/z 810.0 (M^+). Anal. Calc. for $C_{40}H_{46}N_2P_2Pt$: C, 59.18; H, 5.71. Observed: C, 59.21; H, 5.70%.

trans-[R−C≡C-(Bu$_3$P)$_2$Pt−C≡C−R] (R = Carbazole-3-yl), ***M6.*** A similar synthesis to that used to prepare **M3** was followed using **L2** and afforded a pale brown solid (81.6%, mp 187.3 °C). IR (ATR, diamond): ν/cm^{-1} 3397 (N−H), 2097 (−C≡C−). ^{1}H NMR (700 MHz, $CDCl_3$, ppm): δ 8.02−7.96 (m, 4H, H-4, 4′, 5, 5′), 7.42−7.34 (m, 4H, H-1, 1′, 8, 8′), 7.30 (d, J = 7.1 Hz, 2H, H-2, 2′), 7.21 (t, J = 7.0 Hz, 4H, H-6, 6′,7, 7′), 2.24 (br s, 2H, NH, NH′), 1.69−1.65 (m, 12H, PCH_2), 1.80−1.39 (m, 24H, CH_2), 1.14−0.84 (m, 18H, alkyl CH_3). ^{13}C NMR (176 MHz, $CDCl_3$, ppm): δ 139.95, 137.48, 137.43, 129.48, 129.35, 125.77, 123.38, 122.60, 122.46, 120.85, 120.72, 120.34, 119.44, 110.70, 110.19, 109.35 (aromatic), 104.88, 104.86, 104.78, 104.70 (−C≡C−), 26.59−24.08 (alkyl CH_2), 14.85−13.02 (alkyl CH_3). ^{31}P{^{1}H}NMR (122 MHz, $CDCl_3$, ppm): δ 3.37, $^1J_{Pt-P}$ = 2380.2 Hz. ESI-MS: m/z 979.4 (M^+). Anal. Calc. for $C_{52}H_{70}N_2P_2Pt$: C, 63.72; H, 7.20, C. Observed: 63.90; H, 7.21%.

trans-[(Ph)(Et$_3$P)$_2$Pt−C≡C−R−C≡C−Pt(PEt$_3$)$_2$(Ph)] (R = Carbazole-2,7-diyl), ***M7.*** The compound was prepared as previously reported.[11f] ^{1}H NMR (250 MHz, $CDCl_3$, ppm): δ 7.80 (d, J = 7.9 Hz, 4H, H_{ortho} of Ph), 7.42 (d, J = 7.7 Hz, 2H, H-4, 5), 7.32 (s, 2H, H-1, 8), 7.20 (dd, J = 13.9, 7.4 Hz, 2H, H-3, 6), 6.98 (t, J = 7.4 Hz, 4H, H_{meta} of Ph), 6.82 (t, J = 7.3 Hz, 2H, H_{para} of Ph), 5.20 (br s, 1H, NH), 1.80−1.61 (m, 24H, PCH_2), 1.07−0.98 (m, 36H, alkyl CH_3). FAB-MS: *mlz* 1230.2 (M^+).

trans-[(Ph)(Et$_3$P)$_2$Pt−C≡C−R−C≡C−Pt(PEt$_3$)$_2$(Ph)] (R = N-(2-Ethylhexylcarbazole-2,7-diyl)), ***M8.*** The compound was prepared as previously reported.[11f] ^{1}H NMR (250 MHz, $CDCl_3$, ppm): δ 7.81 (d, J = 7.7 Hz, 2H, H-4, 5), 7.35 (d, J = 7.9 Hz, 4H, H_{ortho} of Ph), 7.25 (s, 2H, H-1, 8), 7.14 (dd, J = 13.2, 7.0 Hz, 2H, H-3, 6), 6.97 (t, J = 7.6 Hz, 4H, H_{meta} of Ph), 6.88 (t, J = 8.0 Hz, 2H, H_{para} of Ph), 4.05−4.06 (m, 2H, NCH_2), 1.81−1.78 (m, 24H, PCH_2), 1.62−1.57 (m, 1H, alkyl CH), 1.43−1.38 (m, 8H, alkyl CH_2), 1.20−1.14 (m, 36H, alkyl CH_3), 0.88 (t, J = 7.8 Hz, 6H, alkyl CH_3). FAB-MS: m/z 1342.3 (M^+).

trans-[(Ph)(Et$_3$P)$_2$Pt−C≡C−R−C≡C−Pt(PEt$_3$)$_2$(Ph)] (R = Carbazol-3,6-diyl), ***M9.*** The compound was prepared as previously reported.[11f] ^{1}H NMR (250 MHz, $CDCl_3$, ppm): δ 7.53 (d, J = 7.9 Hz, 2H, H-4, 5), 7.41 (d, J = 8.0 H, 2H, H-2, 7), 7.32 (dd, J = 14.0, 7.4 Hz, 4H, H_{ortho} of Ph), 7.26 (d, J = 8.0 Hz, 2H, H-1, 8), 6.96 (t, J = 7.9 Hz, 4H, H_{meta} of Ph), 6.80 (t, J = 7.9 Hz, 2H, H_{para} of Ph), 9.55 (s, 1H, NH), 1.82−1.75 (m, 24H, PCH_2), 0.86 (t, J = 7.2 Hz, 36H, CH_3). FAB-mass spectrum: m/z 1230.1 (M^+).

trans-[(Ph)(Et$_3$P)$_2$Pt−C≡C−R−C≡C−Pt(PEt$_3$)$_2$(Ph)] (R = N-(2-Ethylhexylcarbazole-3,6-diyl)), ***M10.*** To a stirred mixture of **L4b** (0.150 g, 0.461 mmol) and *trans*-[$Pt(PEt_3)_2PhCl$] (0.543 g, 1.00 mmol) in ^{i}Pr$_2$NH (20 mL) and CH_2Cl_2 (20 mL) was added CuI (1 mg). The solution was stirred at room temperature under Ar over a period of 18 h, after which all volatile components were removed under reduced pressure. The crude product was taken up in CH_2Cl_2 and purified using silica column chromatography with hexane/CH_2Cl_2 (1:1, v/v) as the eluent. The product was obtained as a brown solid (0.480 g, 77.5%). IR (CH_2Cl_2): ν/cm^{-1} 2090 (−C≡C−). ^{1}H NMR (700 MHz, $CDCl_3$, ppm) δ 8.08 (s, 1H, H-4), 7.88 (s, 1H, H-5), 7.48 (dd, J = 8.7, 1.9 Hz, 1H, H-1), 7.40 (ddd, J = 21.9, 8.5, 1.7 Hz, 1H, H-8), 7.29 (d, J = 7.0 Hz, 2H, H-2, 7), 7.17−7.13 (m, 4H, H_{ortho} of Ph), 6.90 (t, J = 7.4 Hz, 4H, H_{meta} of Ph), 6.74 (dd, J = 14.1, 6.9 Hz, 2H, H_{para} of Ph), 3.60−3.56 (m, 2H, NCH_2), 1.99−1.88 (m, 1H, alkyl CH), 1.77−1.65 (m, 24H, PCH_2), 1.34−1.10 (m, 8H, alkyl CH_2), 1.10−0.91 (m, 36H, alkyl CH_3), 0.85−0.69 (m, 6H, alkyl CH_3). ^{13}C NMR (176 MHz, $CDCl_3$, ppm) δ 138.77, 138.28, 137.95, 128.91, 127.98, 126.89, 126.25, 123.42, 122.41, 122.21, 121.96, 121.35, 120.63, 120.13, 110.92 (aromatic), 110.20, 109.67, 109.29, 107.73 (−C≡C−), 52.42, 46.66, 46.52, 38.35, 38.32, 29.97, 29.94, 28.70, 27.81, 27.74, 23.34, 22.03, 21.99, 21.70 (alkyl CH_2), 14.23, 14.14, 14.04, 13.13, 13.03, 12.99, 9.88, 9.86, 7.09, 6.82 (alkyl CH_2).^{31}P{^{1}H}-NMR (101.3 MHz, $CDCl_3$): δ − 131.8, $^1J_{Pt-P}$ = 2637 Hz. FAB-MS: m/z 1342.1 (M^+). Anal. Calc. for $C_{60}H_{93}P_4Pt_2N$: C, 53.69; H, 6.98. Observed: C, 53.72; H, 6.91%.

trans-[(Bu$_3$P)$_2$Pt−C≡C−R−C≡C−]$_n$ (R = Carbazole-2,7-diyl), ***P1.*** The compound was prepared according to the previously reported procedure.[11f] ^{1}H NMR (250 MHz, $CDCl_3$, ppm): δ 7.81 (dd, J = 7.2, 2,2 Hz, 2H, H-4, 5), 7.27 (s, 2H, H-1, 8), 7.15 (d, J = 7.0 Hz, 2H, H-3, 6), 5.65 (s, 1H, NH), 2.18−2.10 (m, 12H, PCH_2), 1.58−1.30 (m, 24H, alkyl CH_2), 1.08−0.87 (m, 18H, alkyl CH_3). GPC (THF): $\bar{M}_n$ = 25 500 g mol^{-1} (n = 31), $\bar{M}_w$= 40 500 g mol^{-1}, PDI = 1.6.

trans-[−(Bu$_3$P)$_2$Pt−C≡C−R−C≡C−]$_n$ (R = N-(2-Ethylhexylcarbazole-2,7-diyl)), ***P2.*** The compound was prepared according to the previously reported procedure.[11f] ^{1}H NMR (250 MHz, $CDCl_3$, ppm): δ 7.83 (d, J = 6.9 Hz, 2H, H-4, 5), 7.21 (s, 2H, H-1, 8), 6.99 (d, J = 7.1 Hz, 2H, H-3, 6), 4.04−4.01 (m, 2H, NCH_2), 2.66−2.57 (m, 1H, alkyl CH), 2.22 (m, 12H, PCH_2), 1.58−1.46 (m, 32H, alkyl CH_2), 1.12−0.90 (m, 24H, alkyl CH_3). GPC (THF): $\bar{M}_n$ = 40 000 g mol^{-1} (n = 43), $\bar{M}_w$ = 72 000 g mol^{-1}, PDI = 1.8.

trans-[−(Bu$_3$P)$_2$Pt−C≡C−R−C≡C−]$_n$ (R = Carbazol-3,6-diyl), ***P3.*** The compound was prepared following the previously reported procedure.[11f] ^{1}H NMR (250 MHz, $CDCl_3$, ppm): δ 7.50 (d, J = 7.7 Hz, 2H, H-4, 5), 7.41 (dd, J = 13.9, 7.4 Hz, 2H, H-1, 8), 7.25 (d, J = 8.2 Hz, 2H, H-2, 7), 5.57 (s, 1H, NH), 2.20−2.01 (m, 12H, PCH_2), 1.67−1.01 (m, 24H, alkyl CH_2), 0.93 (t, J = 7.9 Hz, 18H, alkyl CH_3). GPC (THF): $\bar{M}_n$ = 17 900 g mol^{-1} (n = 22), $\bar{M}_w$= 30 500 g mol^{-1}, PDI = 1.7.

trans-[−(Bu$_3$P)$_2$Pt−C≡C−R−C≡C−]$_n$ (R = N-(2-ethylhexylcarbazole-3,6-diyl)), ***P4.*** The poly-yne was synthesized by mixing **L4b** (0.100 g, 0.305 mmol), *trans*-[$Pt(PBu_3)_2Cl_2$] (0.205 g, 0.305 mmol), and CuI (1 mg) in ^{i}Pr$_2$NH/CH_2Cl_2 (50 mL, 1:1, v/v). After stirring at room temperature overnight under Ar, the solvent was evaporated under reduced pressure. The residue was dissolved in CH_2Cl_2 and

DOI: 10.1021/acs.inorgchem.6b00523
Inorg. Chem. XXXX, XXX, XXX−XXX

filtered through a short alumina column, using hexane/CH_2Cl_2 (1:1, v/v) as eluent, to remove ionic impurities and catalyst residues. After removal of the solvent, the crude product was purified twice by precipitation in CH_2Cl_2 from MeOH. Subsequent washing with hexane and drying *in vacuo* gave a brown solid (0.226 g, 80.1%). IR (CH_2Cl_2): ν/cm^{-1} 2097 (−C≡C−). ^{1}H NMR (700 MHz, $CDCl_3$, ppm) δ 7.94 (s, 2H, H-4, 5), 7.38 (d, J = 8.2 Hz, 2H, H-1, 8), 7.18 (d, J = 8.3 Hz, 2H, H-2, 7), 4.14−4.02 (m, 2H, NCH_2), 3.29 (m, 1H, alkyl CH), 2.21 (t, J = 21.4 Hz, 10H, PCH_2), 2.09−1.99 (m, 2H, PCH_2), 1.75−1.11 (m, 32H, alkyl CH_2), 0.99−0.75 (m, 24H, alkyl CH_3). ^{13}C NMR (176 MHz, $CDCl_3$, ppm) δ 138.07, 127.93, 123.10, 121.53, 121.22, 118.51 (aromatic), 108.27, 107.34 (−C≡C−), 46.27 (NCH_2), 38.35 (alkyl CH), 29.94, 28.70, 27.74, 25.44, 25.34, 25.12, 23.52, 23.49, 23.45, 23.34, 23.09, 22.99, 22.89, 22.05 (alkyl CH_2), 13.02, 12.92, 12.86, 9.90 (alkyl CH_3). ^{31}P{^{1}H}-NMR (101.3 MHz, $CDCl_3$): δ − 137.55, $^1J_{Pt-P}$ = 233 Hz. Anal. Calc. for $[C_{48}H_{77}P_2PtN]_n$: C, 62.31; H, 8.39. Observed: C, 62.20; H, 8.36%. GPC (THF): $\bar{M}_n$ = 36 000 g mol^{-1} (n = 39), $\bar{M}_w$ = 70 000 g mol^{-1}, PDI = 1.9

X-ray Crystallography. The crystals of **3a-TMSA**, **4a-TMSA**, **M3**, and **M7** were mounted in inert oil on glass fibers. Data were measured using Mo Kα radiation (λ = 0.71073 Å) with a Bruker Kappa CCD diffractometer or an Agilent Gemini A-Ultra diffractometer (for **M3**) both equipped with an Oxford Cryostream low-temperature attachment. Structures were solved by direct methods (*SHELXS-86*)[27] and subjected to full-matrix least-squares refinement on F^2 (*SHELXL-97*).[28] In both **M3** and **M7**, there was extensive disorder in the alkyl groups of the phosphine ligands, and in **M7**, two orientations of one of the terminal phenyl groups were also observed. These features were modeled over two or three sites using partial occupancies, summed to unity, and additional constraints were placed on the bond parameters to maintain reasonable bond lengths and angles. In **M7**, the two partially occupied phenyl-ring positions were restrained using the FLAT command. Except for some of the disordered carbon atoms in the alkyl chains of the phosphine ligands, all the nonhydrogen atoms were refined anisotropically. Hydrogen atoms were included using rigid methyl groups or a riding model and, again, partial occupancies were included as appropriate. Refinement continued until convergence was reached, and in the final cycles of refinement, a weighting scheme was introduced that afforded a relatively flat analysis of variance.

Molecular-Weight Measurements. Molar masses were determined by gel-permeation chromatography (GPC),[29] using two PL Gel 30 cm, 5 μm mixed C columns at 30 C, running in THF at 1 cm^3 min^{-1} with a Roth Mocel 200 high-precision pump. A DAWN DSP (Wyatt Technology) multiangle laser-light scattering (MALLS) apparatus with 18 detectors and an auxiliary Viscotek model 200 differential refractometer/viscometer detector was used to calculate the molecular weights (the overall technique is referred to as GPC-LS).

Computational Modeling. Molecular quantum-chemical calculations were carried out using the density-functional theory (DFT) formalism, as implemented in the NWChem code.[30] The B3LYP hybrid functional[31] was used in conjunction with Pople split-valence basis sets[32] of 6-31g and 6-31g** quality for the H and non-H atoms, respectively, and the LANL2DZ pseudopotential[33] and corresponding double-ζ basis set were used to describe Pt. The convergence tolerances for the optimization of the electronic wave functions were set to 10^{-6}, 10^{-5}, and 5×10^{-4} a.u. on the total energy, density, and gradients, respectively. The geometries of the four initial models were optimized until the maximum and root-mean-square (RMS) gradients on the ions were less than 4.5×10^{-4} and 3×10^{-4} a.u., respectively, and the maximum and RMS Cartesian steps in the last iteration fell below 1.8×10^{-3} and 1.2×10^{-3} a.u. The minima were then verified by computing the vibrational frequencies using analytical gradients; during these calculations, the tolerances on the energy, density, and gradients during the electronic minimization were tightened to 10^{-8}, 10^{-6}, and 10^{-5} a.u., respectively. Finally, time-dependent DFT (TD-DFT) calculations were carried out on the optimized models using adiabatic B3LYP. The 50 lowest-lying singlet (spin-allowed) and triplet (spin-forbidden) electronic excitations were computed, and the former were used to generate a simulated UV/vis absorption spectrum according to the equation:

$$\varepsilon(\nu) = \sum_i 1.3062974 \times 10^8 \frac{f_i}{\sigma} \exp\left(-\left[\frac{\nu - \nu_i}{\sigma}\right]^2\right)$$

where the energies, ν, are in wavenumbers (cm^{-1}), ε is the molar extinction coefficient in L mol^{-1} cm^{-1}, f_i is the (dimensionless) oscillator strength, ν_i is the band position, and σ is a uniform bandwidth used to broaden the peaks, here set to 0.2 eV.

■ ASSOCIATED CONTENT

Supporting Information

The Supporting Information is available free of charge on the ACS Publications website at DOI: 10.1021/acs.inorgchem.6b00523.

CCDC reference numbers 1456923−1456926.(CIF)

■ AUTHOR INFORMATION

Corresponding Authors

*E-mail: msk@squ.edu.om.
*E-mail: j.m.skelton@bath.ac.uk.
*E-mail: p.r.raithby@bath.ac.uk.

Notes

The authors declare no competing financial interest.

■ ACKNOWLEDGMENTS

M.S.K. gratefully acknowledges the Research Council (TRC), Oman for funding (grant no. ORG/EI/SQU/13/015). This work was conducted as part of a Strategic Project submitted to Sultan Qaboos University (SQU), Oman for funding from His Majesty's Trust Fund (HMTF). R.A.A.-B. acknowledges SQU for a PhD scholarship and M.S.K. for a research leave. J.M.S. and P.R.R. are supported by an EPSRC programme grant (grant no. EP/K004956/1). The computational modelling was carried out using the UK Archer facility, accessed through the UK Materials Chemistry Consortium, which is funded by the EPSRC (grant no. EP/L000202). Some modelling was also performed using the Balena HPC system at the University of Bath, which is maintained by Bath University Computing Services.

■ REFERENCES

(1) (a) Dong, H.; Zhu, H.; Meng, Q.; Gong, X.; Hu, W. *Chem. Soc. Rev.* **2012**, *41*, 1754. (b) Joachim, C.; Gimzewski, J.; Aviram, A. *Nature* **2000**, *408*, 541. (c) Williams, K. A.; Boydston, A. J.; Bielawski, C. W. *Chem. Soc. Rev.* **2007**, *36*, 729. (d) Zhou, G.-J.; Wong, W.-Y. *Chem. Soc. Rev.* **2011**, *40*, 2541.

(2) (a) Zhou, J.; Whittell, G. R.; Manners, I. *Macromolecules* **2014**, *47*, 3529. (b) Xu, H.; Chen, R.; Sun, Q.; Lai, W.; Su, Q.; Huang, W.; Liu, X. *Chem. Soc. Rev.* **2014**, *43*, 3259. (c) Wong, W.-Y.; Harvey, P. D. *Macromol. Rapid Commun.* **2010**, *31*, 671. (d) Whittell, G. R.; Hager, M. D.; Schubert, U. S.; Manners, I. *Nat. Mater.* **2011**, *10*, 176. (e) Abd-El-Aziz, A. S.; Strohm, E. A. *Polymer* **2012**, *53*, 4879.

(3) (a) Wong, W.-Y. *Dalton Trans.* **2007**, 4495. (b) Wong, W.-Y.; Ho, C.-L. *Coord. Chem. Rev.* **2006**, *250*, 2627. (c) Wong, W.-Y. *Coord. Chem. Rev.* **2005**, *249*, 971. (d) Khan, M. S.; Al-Suti, M. K.; Maharaja, J.; Haque, A.; Al-Balushi, R.; Raithby, P. R. *J. Organomet. Chem.* **2015**, DOI: 10.1016/j.jorganchem.2015.10.003. (e) Ho, C.-L.; Wong, W.-Y. *Coord. Chem. Rev.* **2011**, *255*, 2469. (f) Ho, C.-L.; Wong, W.-Y. *Coord. Chem. Rev.* **2013**, *257*, 1614.

(4) (a) Yam, V. W. *Nat. Chem.* **2010**, *2*, 790. (b) Wilson, J.; Kohler, A.; Friend, R.; Al-Suti, M.; Al-Mandhary, M.; Khan, M.; Raithby, P. *J. Chem. Phys.* **2000**, *113*, 7627. (c) Khan, M. S.; Al-Mandhary, M. R.; Al-Suti, M. K.; Hisahm, A. K.; Raithby, P. R.; Ahrens, B.; Mahon, M. F.;

DOI: 10.1021/acs.inorgchem.6b00523
Inorg. Chem. XXXX, XXX, XXX−XXX

Male, L.; Marseglia, E. A.; Tedesco, E.; et al. *J. Chem. Soc., Dalton Trans.* **2002**, 1358−1368. (d) Khan, M. S.; Al-Mandhary, M. R.; Al-Suti, M. K.; Feeder, N.; Nahar, S.; Köhler, A.; Friend, R. H.; Wilson, P. J.; Raithby, P. R. *J. Chem. Soc., Dalton Trans.* **2002**, 2441. (e) Khan, M. S.; Al-Mandhary, M. R.; Al-Suti, M. K.; Ahrens, B.; Mahon, M. F.; Male, L.; Raithby, P. R.; Boothby, C. E.; Köhler, A. *Dalton Trans.* **2003**, 74.

(5) (a) Silvestri, F.; Marrocchi, A. *Int. J. Mol. Sci.* **2010**, *11*, 1471. (b) Wilson, J. S.; Chawdhury, N.; Al-Mandhary, M. R.; Younus, M.; Khan, M. S.; Raithby, P. R.; Köhler, A.; Friend, R. H. *J. Am. Chem. Soc.* **2001**, *123*, 9412. (c) Chawdhury, N.; Köhler, A.; Friend, R.; Wong, W.-Y.; Lewis, J.; Younus, M.; Raithby, P.; Corcoran, T.; Al-Mandhary, M.; Khan, M. *J. Chem. Phys.* **1999**, *110*, 4963. (d) Köhler, A.; Wittmann, H.; Friend, R.; Khan, M.; Lewis, J. *Synth. Met.* **1996**, *77*, 147. (e) Liu, L.; Wong, W.-Y.; Shi, J.-X.; Cheah, K.-W. *J. Polym. Sci., Part A: Polym. Chem.* **2006**, *44*, 5588.

(6) Wilson, J.; Dhoot, A.; Seeley, A.; Khan, M.; Köhler, A.; Friend, R. *Nature* **2001**, *413*, 828.

(7) Aly, S. M.; Ho, C. L.; Fortin, D.; Wong, W. Y.; Abd-El-Aziz, A. S.; Harvey, P. D. *Chem. - Eur. J.* **2008**, *14*, 8341.

(8) (a) Du, J.; Fang, Q.; Bu, D.; Ren, S.; Cao, A.; Chen, X. *Macromol. Rapid Commun.* **2005**, *26*, 1651. (b) Liu, L.; Wong, W.-Y.; Shi, J.-X.; Cheah, K.-W.; Lee, T.-H.; Leung, L. M. *J. Organomet. Chem.* **2006**, *691*, 4028. (c) Liu, Y.-L.; Yu, J.-M. *J. Polym. Sci., Part A: Polym. Chem.* **2006**, *44*, 1890. (d) Ho, C.-L.; Chui, C.-H.; Wong, W.-Y.; Aly, S. M.; Fortin, D.; Harvey, P. D.; Yao, B.; Xie, Z.; Wang, L. *Macromol. Chem. Phys.* **2009**, *210*, 1786.

(9) (a) Cornil, J.; Dos Santos, D.; Crispin, X.; Silbey, R.; Brédas, J.-L. *J. Am. Chem. Soc.* **1998**, *120*, 1289. (b) Bunz, U. H.; Enkelmann, V.; Kloppenburg, L.; Jones, D.; Shimizu, K. D.; Claridge, J. B.; zur Loye, H.-C.; Lieser, G. *Chem. Mater.* **1999**, *11*, 1416.

(10) (a) Jiang, H.; Sun, J.; Zhang, J. *Curr. Org. Chem.* **2012**, *16*, 2014. (b) Kato, S.-i.; Noguchi, H.; Kobayashi, A.; Yoshihara, T.; Tobita, S.; Nakamura, Y. *J. Org. Chem.* **2012**, *77*, 9120. (c) Mizuno, Y.; Takasu, I.; Uchikoga, S.; Enomoto, S.; Sawabe, T.; Amano, A.; Wada, A.; Sugizaki, T.; Yoshida, J.; Ono, T.; et al. *J. Phys. Chem. C* **2012**, *116*, 20681. (d) Grimsdale, A. C.; Leok Chan, K.; Martin, R. E.; Jokisz, P. G.; Holmes, A. B. *Chem. Rev.* **2009**, *109*, 897. (e) Grazulevicius, J.; Strohriegl, P.; Pielichowski, J.; Pielichowski, K. *Prog. Polym. Sci.* **2003**, *28*, 1297. (f) Morin, J.-F.; Leclerc, M.; Ades, D.; Siove, A. *Macromol. Rapid Commun.* **2005**, *26*, 761. (g) Li, J.; Grimsdale, A. C. *Chem. Soc. Rev.* **2010**, *39*, 2399.

(11) (a) Wong, W.-Y.; Lu, G.-L.; Choi, K.-H.; Shi, J.-X. *Macromolecules* **2002**, *35*, 3506. (b) Tao, C.-H.; Wong, K. M.-C.; Zhu, N.; Yam, V. W.-W. *New J. Chem.* **2003**, *27*, 150. (c) Liu, L.; Wong, W.-Y.; Poon, S.-Y.; Cheah, K.-W. *J. Inorg. Organomet. Polym. Mater.* **2005**, *15*, 555. (d) Ho, C.-L.; Wong, W.-Y. *J. Organomet. Chem.* **2006**, *691*, 395. (e) Khan, M. S.; Al-Saadi, R. K.; Male, L.; Raithby, P. R.; Bjernemose, J. K. *Acta Crystallogr., Sect. E: Struct. Rep. Online* **2003**, *59*, 774. (f) Zhang, N.; Hayer, A.; Al-Suti, M. K.; Al-Belushi, R. A.; Khan, M. S.; Köhler, A. *J. Chem. Phys.* **2006**, *124*, 244701.

(12) (a) Patrick, D.; Boykin, D.; Wilson, W.; Tanious, F.; Spychala, J.; Bender, B.; Hall, J.; Dykstra, C.; Ohemeng, K.; Tidwell, R. *Eur. J. Med. Chem.* **1997**, *32*, 781. (b) Seneclauze, J. B.; Retailleau, P.; Ziessel, R. *New J. Chem.* **2007**, *31*, 1412.

(13) Yang, C.-J.; Chang, Y. J.; Watanabe, M.; Hon, Y.-S.; Chow, T. J. *J. Mater. Chem.* **2012**, *22*, 4040.

(14) Khan, M. S.; Al-Suti, M. K.; Al-Mandhary, M. R.; Ahrens, B.; Bjernemose, J. K.; Mahon, M. F.; Male, L.; Raithby, P. R.; Friend, R. H.; Köhler, A.; et al. *Dalton Trans.* **2003**, 65.

(15) (a) Nayak, M. K.; Dogra, S. K. *J. Photochem. Photobiol., A* **2004**, *161*, 169. (b) Li, W.; Zheng, H.; Ye, C.; Wu, T.; Fan, M.; Feng, J. *Energy Fuels* **2012**, *26*, 6316.

(16) (a) Khan, M. S.; Al-Mandhary, M. R.; Al-Suti, M. K.; Hisahm, A. K.; Raithby, P. R.; Ahrens, B.; Mahon, M. F.; Male, L.; Marseglia, E. A.; Tedesco, E.; et al. *J. Chem. Soc. Dal. Trans.* **2002**, 1358. (b) Khan, M. S.; Al-Mandhary, M. R.; Al-Suti, M. K.; Al-Battashi, F. R.; Al-Saadi, S.; Ahrens, B.; Bjernemose, J. K.; Mahon, M. F.; Raithby, P. R.; Younus, M.; et al. *Dalton Trans.* **2004**, 2377.

(17) (a) Lambert, J. B.; Shurvell, H. F.; Lightner, D. A.; Cooks, R. G. *Introduction to organic spectroscopy*; Macmillan Publishing Company: New York, 1987. (b) Manna, J.; John, K. D.; Hopkins, M. D. *Adv. Organomet. Chem.* **1995**, *38*, 79.

(18) (a) Khan, M. S.; Al-Suti, M. K.; Shah, H. H.; Al-Humaimi, S.; Al-Battashi, F. R.; Bjernemose, J. K.; Male, L.; Raithby, P. R.; Zhang, N.; Köhler, A.; et al. *Dalton Trans.* **2011**, *40*, 10174. (b) Liu, R.; Chen, H.; Chang, J.; Li, Y.; Zhu, H.; Sun, W. *Dalton Trans.* **2013**, *42*, 160. (c) Wu, P.-T.; Bull, T.; Kim, F. S.; Luscombe, C. K.; Jenekhe, S. A. *Macromolecules* **2009**, *42*, 671.

(19) Aly, S. M.; Ho, C.-L.; Wong, W.-Y.; Fortin, D.; Harvey, P. D. *Macromolecules* **2009**, *42*, 6902.

(20) Khan, M. S.; Male, L.; Raithby, P. R.; Teat, S. J.; Bond, A. D. *Acta Crystallogr., Sect. E: Struct. Rep. Online* **2003**, *59*, 1342.

(21) Becke, A. D. *J. Chem. Phys.* **1993**, *98*, 1372.

(22) Momma, K.; Izumi, F. *J. Appl. Crystallogr.* **2011**, *44*, 1272.

(23) Armarego, W. L.; Chai, C. L. L. *Purification of laboratory chemicals*; Butterworth-Heinemann: Boston, 2013.

(24) Yamato, T.; Hideshima, C.; Suehiro, K.; Tashiro, M.; Prakash, G. S.; Olah, G. A. *J. Org. Chem.* **1991**, *56*, 6248.

(25) Siegmann, K.; Pregosin, P. S.; Venanzi, L. M. *Organometallics* **1989**, *8*, 2659.

(26) Kauffman, G. B.; Teter, L. A.; Huheey, J. E. *Inorg. Synth.* **1963**, *7*, 245.

(27) Sheldrick, G. M. *SHELXS-86, Program for Crystal Structure Solution*; University of Göttingen: Germany, 1986.

(28) Sheldrick, G. M. *Acta Crystallogr., Sect. A: Found. Crystallogr.* **2008**, *A64*, 112.

(29) (a) Charles, E., Jr. *Organometallic polymers*; Elsevier: New York, 2012. (b) Takahashi, S.; Kariya, M.; Yatake, T.; Sonogashira, K.; Pittman, C. U. J. *Organometallic Polymers*; Academic Press: New York, 1978.

(30) Valiev, M.; Bylaska, E. J.; Govind, N.; Kowalski, K.; Straatsma, T. P.; Van Dam, H. J.; Wang, D.; Nieplocha, J.; Apra, E.; Windus, T. L.; et al. *Comput. Phys. Commun.* **2010**, *181*, 1477.

(31) Becke, A. D. *J. Chem. Phys.* **1993**, *98*, 1372.

(32) Ditchfield, R.; Hehre, W. J.; Pople, J. A. *J. Chem. Phys.* **1971**, *54*, 724.

(33) Hay, P. J.; Wadt, W. R. *J. Chem. Phys.* **1985**, *82*, 270.

DOI: 10.1021/acs.inorgchem.6b00523
Inorg. Chem. XXXX, XXX, XXX−XXX